Design of Even-Order Complex Wave Digital Filters

by

Jin Wang

A Thesis

Presented to the Faculty of Graduate Studies

in Partial Fulfillment of the Requirements

for the Degree

MASTER OF SCIENCE

Department of Electrical and Computer Engineering

University of Manitoba

Winnipeg, Manitoba

SEPTEMBER, 1996

ISBN 0-612-16365-2

Canada

Name _____

Dissertation Abstracts International and *Masters Abstracts International* are arranged by broad, general subject categories. Please select the one subject which most nearly describes the content of your dissertation or thesis. Enter the corresponding four-digit code in the spaces provided.

SUBJECT TERM

Engineering, Electronics and Electrical

0544 UMI

SUBJECT CODE

Subject Categories

THE HUMANITIES AND SOCIAL SCIENCES

COMMUNICATIONS AND THE ARTS
Architecture 0729
Art History 0377
Cinema 0900
Dance 0378
Design and Decorative Arts 0389
Fine Arts 0357
Information Science 0723
Journalism 0391
Landscape Architecture 0390
Library Science 0399
Mass Communications 0708
Music 0413
Speech Communication 0459
Theater 0465

EDUCATION
General 0515
Administration 0514
Adult and Continuing 0516
Agricultural 0517
Art 0273
Bilingual and Multicultural 0282
Business 0688
Community College 0275
Curriculum and Instruction 0727
Early Childhood 0518
Elementary 0524
Educational Psychology 0525
Finance 0277
Guidance and Counseling 0519
Health 0680
Higher 0745
History of 0520
Home Economics 0278
Industrial 0521
Language and Literature 0279
Mathematics 0280
Music 0522
Philosophy of 0998
Physical 0523
Reading 0535
Religious 0527
Sciences 0714
Secondary 0533
Social Sciences 0534
Sociology of 0340
Special 0529
Teacher Training 0530
Technology 0710
Tests and Measurements 0288
Vocational 0747

LANGUAGE, LITERATURE AND LINGUISTICS
Language
- General 0679
- Ancient 0289
- Linguistics 0290
- Modern 0291
- Rhetoric and Composition 0681

Literature
- General 0401
- Classical 0294
- Comparative 0295
- Medieval 0297
- Modern 0298
- African 0316
- American 0591
- Asian 0305
- Canadian (English) 0352
- Canadian (French) 0355
- Caribbean 0360
- English 0593
- Germanic 0311
- Latin American 0312
- Middle Eastern 0315
- Romance 0313
- Slavic and East European 0314

PHILOSOPHY, RELIGION AND THEOLOGY
Philosophy 0422
Religion
- General 0318
- Biblical Studies 0321
- Clergy 0319
- History of 0320
- Philosophy of 0322

Theology 0469

SOCIAL SCIENCES
American Studies 0323
Anthropology
- Archaeology 0324
- Cultural 0326
- Physical 0327

Business Administration
- General 0310
- Accounting 0272
- Banking 0770
- Management 0454
- Marketing 0338

Canadian Studies 0385
Economics
- General 0501
- Agricultural 0503
- Commerce-Business 0505
- Finance 0508
- History 0509
- Labor 0510
- Theory 0511

Folklore 0358
Geography 0366
Gerontology 0351
History
- General 0578
- Ancient 0579
- Medieval 0581
- Modern 0582
- Church 0330
- Black 0328
- African 0331
- Asia, Australia and Oceania 0332
- Canadian 0334
- European 0335
- Latin American 0336
- Middle Eastern 0333
- United States 0337

History of Science 0585
Law 0398
Political Science
- General 0615
- International Law and Relations 0616
- Public Administration 0617

Recreation 0814
Social Work 0452
Sociology
- General 0626
- Criminology and Penology 0627
- Demography 0938
- Ethnic and Racial Studies 0631
- Individual and Family Studies 0628
- Industrial and Labor Relations 0629
- Public and Social Welfare 0630
- Social Structure and Development 0700
- Theory and Methods 0344

Transportation 0709
Urban and Regional Planning 0999
Women's Studies 0453

THE SCIENCES AND ENGINEERING

BIOLOGICAL SCIENCES
Agriculture
- General 0473
- Agronomy 0285
- Animal Culture and Nutrition 0475
- Animal Pathology 0476
- Fisheries and Aquaculture 0792
- Food Science and Technology 0359
- Forestry and Wildlife 0478
- Plant Culture 0479
- Plant Pathology 0480
- Range Management 0777
- Soil Science 0481
- Wood Technology 0746

Biology
- General 0306
- Anatomy 0287
- Animal Physiology 0433
- Biostatistics 0308
- Botany 0309
- Cell 0379
- Ecology 0329
- Entomology 0353
- Genetics 0369
- Limnology 0793
- Microbiology 0410
- Molecular 0307
- Neuroscience 0317
- Oceanography 0416
- Plant Physiology 0817
- Veterinary Science 0778
- Zoology 0472

Biophysics
- General 0786
- Medical 0760

EARTH SCIENCES
Biogeochemistry 0425
Geochemistry 0996
Geodesy 0370
Geology 0372
Geophysics 0373
Hydrology 0388
Mineralogy 0411
Paleobotany 0345
Paleoecology 0426
Paleontology 0418
Paleozoology 0985
Palynology 0427
Physical Geography 0368
Physical Oceanography 0415

HEALTH AND ENVIRONMENTAL SCIENCES
Environmental Sciences 0768
Health Sciences
- General 0566
- Audiology 0300
- Dentistry 0567
- Education 0350
- Administration, Health Care 0769
- Human Development 0758
- Immunology 0982
- Medicine and Surgery 0564
- Mental Health 0347
- Nursing 0569
- Nutrition 0570
- Obstetrics and Gynecology 0380
- Occupational Health and Safety 0354
- Oncology 0992
- Ophthalmology 0381
- Pathology 0571
- Pharmacology 0419
- Pharmacy 0572
- Public Health 0573
- Radiology 0574
- Recreation 0575
- Rehabilitaion and Therapy 0382
- Speech Pathology 0460
- Toxicology 0383

Home Economics 0386

PHYSICAL SCIENCES
Pure Sciences
Chemistry
- General 0485
- Agricultural 0749
- Analytical 0486
- Biochemistry 0487
- Inorganic 0488
- Nuclear 0738
- Organic 0490
- Pharmaceutical 0491
- Physical 0494
- Polymer 0495
- Radiation 0754

Mathematics 0405
Physics
- General 0605
- Acoustics 0986
- Astronomy and Astrophysics 0606
- Atmospheric Science 0608
- Atomic 0748
- Condensed Matter 0611
- Electricity and Magnetism 0607
- Elementary Particles and High Energy 0798
- Fluid and Plasma 0759
- Molecular 0609
- Nuclear 0610
- Optics 0752
- Radiation 0756

Statistics 0463

Applied Sciences
Applied Mechanics 0346
Computer Science 0984
Engineering
- General 0537
- Aerospace 0538
- Agricultural 0539
- Automotive 0540
- Biomedical 0541
- Chemical 0542
- Civil 0543
- Electronics and Electrical 0544
- Environmental 0775
- Industrial 0546
- Marine and Ocean 0547
- Materials Science 0794
- Mechanical 0548
- Metallurgy 0743
- Mining 0551
- Nuclear 0552
- Packaging 0549
- Petroleum 0765
- Sanitary and Municipal 0554
- System Science 0790

Geotechnology 0428
Operations Research 0796
Plastics Technology 0795
Textile Technology 0994

PSYCHOLOGY
General 0621
Behavioral 0384
Clinical 0622
Cognitive 0633
Developmental 0620
Experimental 0623
Industrial 0624
Personality 0625
Physiological 0989
Psychobiology 0349
Psychometrics 0632
Social 0451

THE UNIVERSITY OF MANITOBA

FACULTY OF GRADUATE STUDIES

COPYRIGHT PERMISSION

DESIGN OF EVEN-ORDER COMPLEX WAVE DIGITAL FILTERS

BY

JIN WANG

A Thesis/Practicum submitted to the Faculty of Graduate Studies of the University of Manitoba in partial fulfillment of the requirements for the degree of

MASTER OF SCIENCE

I hereby declare that I am the sole author of this thesis.

I authorize the University of Manitoba to lend this thesis to other institutions or individuals for the purpose of scholarly research.

Jin Wang

I further authorize the University of Manitoba to reporduce this thesis by photocopying or by other means, in total or in part, at the request of other institutions or individuals for the purpose of scholarly research.

Jin Wang

Acknowledgments

I would like to express my sincere gratitude to Professor G.O. Martens for his encouragement, patience, and ever-helpful guidance throughout the course of this work. I have greatly benefited from his expertise and constant help and advice, without which this work could not have been possible.

Special thanks to my family and friends for their support.

Abstract

This thesis is concerned with complex wave digital filter (WDF) realizations of the most common classical lowpass filters such as Butterworth, Chebyshev and Cauer (elliptic) filters. The direct design method of Gazsi [8] based on lattice WDFs which applies to odd-order lowpass filters is summarized in detail. That method is then generalized to even-order lowpass filters using the theory of complex lattice WDFs. In this regard, an even-order lowpass transfer function is decomposed into two complex allpass functions giving a lattice configuration and each lattice branch is realized by cascaded complex first-degree allpass sections. Two realizations of complex first-degree allpass sections are presented, one with a real two-port terminated by a modular multiplier in series with a delay and the other with a cross structure terminated in a delay. The cross structure (adaptor) has the property that it remains pseudolossless with the quantization of the multiplier coefficients. Using available explicit formulas, a direct design method and some design examples are given for even-order Butterworth, Chebyshev and Cauer(elliptic) filters. The design process includes an optimization of the wordlength (the number of digits) used in the coefficients.

Table of contents

Chapter 1

Introduction

A digital filter is a computational structure derived from a difference equation that produces an output discrete signal (output sequence) from an input discrete signal (input sequence). Each digital filter simulates a linear, shift-invariant discrete time system and is specified by an input-output relationship in either the time or the frequency domain, that filters out a given frequncy range and passes the remaining frequency range (called the passband). The computational structure can be implemented by either a computer program on a general-purpose computer or by a dedicated single chip realization.

Because digital filters are only implemented in a finite precision arithmetic, signal and system coefficients must be approximated, and errors can arise from coefficient quantization, rounding errors and overflow. These errors are termed finite-word-length (FWL) effects. It is well known [1], [22] that a digital filter structure that has low passband sensitivity to coefficient quantizations also generates low level rounding noise. Therefore, in designing a digital filter, a structure with low passband sensitivity to coefficient quantizations is preferred. Otherwise, higher accuracy and longer wordlength have to be used. Unfortunately, the traditional method of direct realization of the transfer function $H(z)$, which uses the coefficients of $H(z)$ as the actual multipliers, suffers from high sensitiv-

ity to coefficients and other FWL effects. There have been several methods developed to reduce FWL effects but the choice is usually difficult due to several available tradeoffs in these approaches.

An alternative to the conventional approach is the wave digital filter (WDF) approach, introduced by Fettweis [1]. WDFs are modeled on classical analog filters (called reference filters) in lattice or ladder configurations, but use wave quantities as the signal variables. Because resistively terminated lossless analog networks have low sensitivity to coefficients, the same properties are carried over to WDFs. Specifically, properly designed WDFs preserve some of the good properties of passive lossless reference filters and have, for example, low passband sensitivity properties which reduce the accuracy requirement and thus the wordlength needed for the multiplier coefficients and also lead to good dynamic range performance. In addition, they have excellent stability properties even under nonliner operating conditions resulting from overflow and roundoff effects. We refer to the review paper by Fettweis [1] and the references contained therein for a detailed discussion of WDFs and their advantages.

While there are many different possible structures for WDF realizations of the classical reference filters, it is well known that explicit formulas exist for some of the structures, which make the design process direct and simple. This is particularly useful for non-expert designers who are not familiar with the intricate techniques of the classical network theory used in the design process. Using some explict formulas available for the most common lowpass filters (Butterworth, Chebyshev and Cauer (elliptic) filters), Gazsi [8] presented a direct design method for lattice WDFs where both lattice branches are realized by cascaded first- and second-degree allpass sections. All coefficients are computed

directly from the design parameters. We note that this method applies to the odd-order classical reference filters only, because an even-order filter cannot be implemented by real lattice WDFs (see [14]).

For an even-order low-pass transfer function (in the z-variable), Vaidyanathan, Regalia and Mitra [14] introduced a method that decomposes it into two complex allpass functions giving a lattice configuration. From this structure and a generalization of WDF to the complex domain, Scarth and Martens [3] presented a complex WDF realization of even-order classical reference filters (such as the Butterworth, Chebyshev and Cauer filters) by implementing the complex allpass function in each lattice branch through an extraction process with complex two-port adaptors and delays.

In this thesis, even-order classical filters will be implemented in lattice complex WDFs (CWDFs) where both lattice branches are realized by cascaded complex first-degree allpass sections. A direct design method will be given for even-order classical reference filters such as the Butterworth, Chebyshev and Cauer filters. The design process includes an optimization of the wordlength (the number of digits) used in the coefficients. In comparison with the method of Scarth and Martens [3], where the complex allpass function in each lattice branch is implemented by recursively extracting a lower degree allpass function, the cascade approach to be presented here is more direct and straightforward. In particular, the implementation of a first-degree allpass section in the cross structure leads to a single coefficient [10], which is very useful in the optimization of wordlength and maintains the pseudolossless of the structure.

In Chapter 2, we briefly describe the real WDFs in the lattice structure and the method used in [8] to realize odd-order classical filters. The implementations of first- and second-

degree allpass sections by means of three-port circulators will be presented in detail, and in Chapter 3 it will be generalized to the complex case.

Our main results are given in Chapter 3. First, in Section 3.1, we describe the method of [14] that decomposes an even-order low-pass transfer function into two complex all-pass functions in lattice structure. Then a corresponding CWDF theory is given in Section 3.2. Section 3.3 gives the realization of a degree one allpass section by complex adaptors. Section 3.4 describes transformations between the variables. Section 3.5 presents synthesis using cascaded allpass sections. Finally, in Section 3.6, a process to optimize the word-length of the cross adaptor coefficients is given.

In Chapter 4, we give the design procedure and examples, and in Chapter 5 the conclusions.

Chapter 2

A direct design method for real WDF

The main purpose of this thesis is to present a complex lattice WDF realization for even order classical lowpass filters and a direct design method (see Chapter 3). This is a generalization of the method in [8], which is described in detail in this chapter. In [8], a direct design method is given for lattice WDF realizations, where both lattice branches are realized by cascaded first- and second-degree allpass sections with real coefficients. Odd-order lowpass digital Butterworth, Chebyshev, and Cauer filters can be implemented using this method.

2.1 Structure of the lattic realization

WDFs are derived from real lossless reference filters using voltage wave quantities [2]. Consider a two-port (Figure 2.1) where for port i (i=1 or 2), the voltage is V_i, the current I_i, and the port (or normalizing) resistance R_i.

Then the the incident and reflected wave quantities A_i and B_i, and the incident and reflected wave vectors are defined by

$$A_i = V_i + R_i I_i, \qquad B_i = V_i - R_i I_i, \qquad i = 1, 2 \tag{2.1a}$$

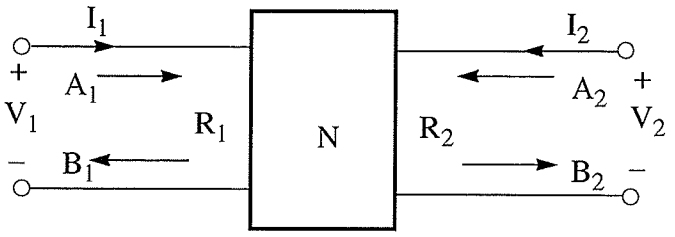

Fig.2.1 A two-port N with port resistances R_1 and R_2

and

$$\boldsymbol{a} = \begin{bmatrix} A_1 \\ A_2 \end{bmatrix} \qquad \boldsymbol{b} = \begin{bmatrix} B_1 \\ B_2 \end{bmatrix} \tag{2.1b}$$

The incident and reflected wave vectors are related by the scattering equation [15]

$$\boldsymbol{b} = \boldsymbol{S}\boldsymbol{a} \tag{2.2}$$

where $\boldsymbol{S}$ is called the scattering matrix:

$$\boldsymbol{S} = \begin{bmatrix} s_{11} & s_{12} \\ s_{21} & s_{22} \end{bmatrix} \tag{2.3}$$

We assume that the two-port N is symmetric and reciprocal, i.e.

$$s_{11} = s_{22} \ , \qquad s_{12} = s_{21} \tag{2.4}$$

Next, define reflections $S_1 = s_{11} - s_{21}$, $S_2 = s_{11} + s_{21}$. In view of (2.3) and (2.1b), the individual equations of (2.2) can be written [15] as

$$2B_1 = S_1 (A_1 - A_2) + S_2 (A_1 + A_2) \tag{2.5}$$

$$2B_2 = -S_1 (A_1 - A_2) + S_2 (A_1 + A_2) \tag{2.6}$$

These equations lead to the Lattice realization of a WDF shown in the following Figure 2.2(a) (with the wave quantities as the input and output)

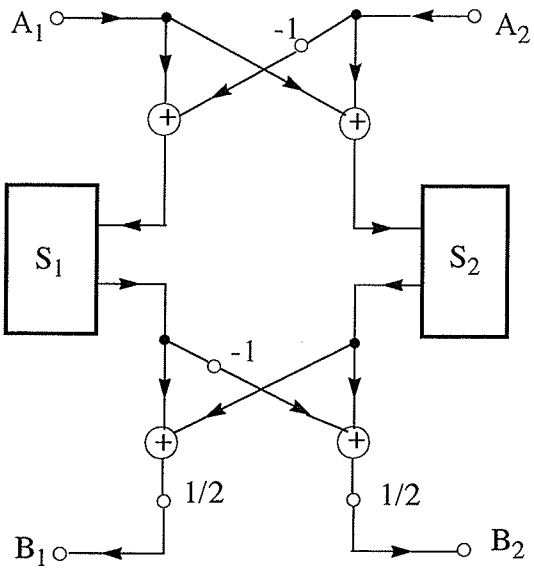

(a)

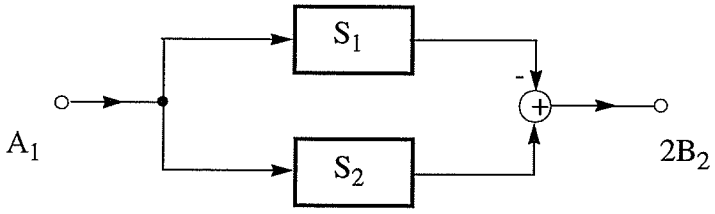

(b)

Fig. 2.2 (a) Wave-flow diagram of a lattice WDF.
(b) Simplified wave-flow diagram.

The correspondence between a WDF and its reference filter is established in the frequency domain, not in the time domain. However, we can not simply carry over the complex frequency p from the reference to the digital domain since, in the latter, transfer functions are not rational in p. Hence, a complex frequency variable, ψ, is usually

adopted. The simplest and most appropriate choice for ψ is the bilinear transform of the z-variable, i.e.,

$$\psi = \frac{z-1}{z+1} = \tanh\left((pT)/2\right), \qquad z = e^{pT} \tag{2.7a}$$

$$T = 1/F \tag{2.7b}$$

where F is the sampling frequency.

In both lattice branches of the lattice WDF (Figure 2.2), $S_1(\psi)$ and $S_2(\psi)$ are all-pass functions. Consequently, they may be written (except for possible sign reversals) in the following form [8]:

$$S_1 = \frac{g_1(-\psi)}{g_1(\psi)} \tag{2.8a}$$

and

$$S_2 = \frac{g_2(-\psi)}{g_2(\psi)} \tag{2.8b}$$

where $g_1(\psi)$ and $g_2(\psi)$ are so called Hurwitz polynomials[24] of degree N_1 and N_2.

Further, the transfer functions that are realized by these WDFs are given by

$$s_{11} = s_{22} = \frac{S_1 + S_2}{2} = \frac{h(\psi)}{g(\psi)} \tag{2.9}$$

$$s_{12} = s_{21} = \frac{S_2 - S_1}{2} = \frac{f(\psi)}{g(\psi)} \tag{2.10}$$

where $h(\psi)$, $f(\psi)$ and $g(\psi)$ are the so-called canonic polynomials [23], [24].

From (2.8), (2.9), and (2.10) we see that

$$g(\psi) = g_1(\psi)\, g_2(\psi) \tag{2.11a}$$

$$h(\psi) = \frac{1}{2}\{g_1(-\psi)g_2(\psi) + g_1(\psi)g_2(-\psi)\} \qquad (2.11b)$$

$$f(\psi) = \frac{1}{2}\{g_1(\psi)g_2(-\psi) - g_1(-\psi)g_2(\psi)\} \qquad (2.11c)$$

$g(\psi)$ is a Hurwitz polynomial of degree N, where $N = N_1 + N_2$.

The degree of the lattice WDF is the sum of the degrees of the two reflectances S_1 and S_2. For the case of real coefficients, N must always be an odd number [15].

It is also known that the zeros of the polynomials $g_1(\psi)$ and $g_2(\psi)$ are alternately distributed in a [8] (see Figure 2.3). This property allows the determination of $g_1(\psi)$ and $g_2(\psi)$ from $g(\psi)$.

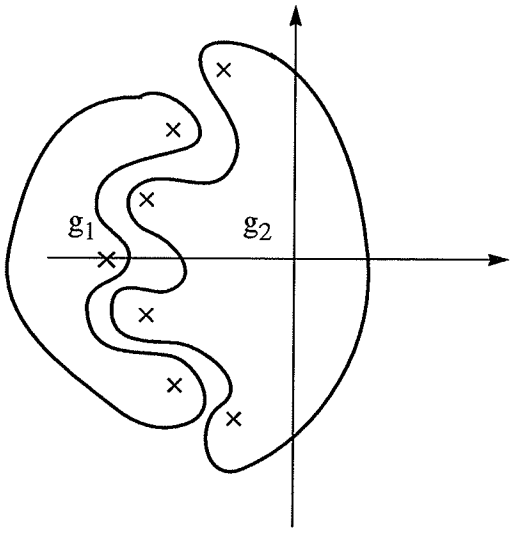

Fig. 2.3. Alternating distribution of the zeros of the polynomial g_1 and g_2.

2.2 Design of lattice WDF

In this section we discuss how to realize allpass functions S_1 and S_2. An allpass function can be synthesized by several different methods. Here, let us consider the realization as a cascade of elementary sections by means of three-port circulators [2]. We consider the elementary sections of first- and second-degree.

2.2.1 The determination of the multiplier coefficient of a section of degree one

A section of degree one has a reflectance of the form:

$$S = \frac{-\psi + B_0}{\psi + B_0} \quad . \tag{2.12}$$

It is known, and we prove below, that, using two-port adaptors, the corresponding wave digital realization has an equivalent wave-flow diagram as shown in Figure 2.4, where the coefficient γ_0 is

$$\gamma_0 = \frac{1 - B_0}{1 + B_0} \tag{2.13}$$

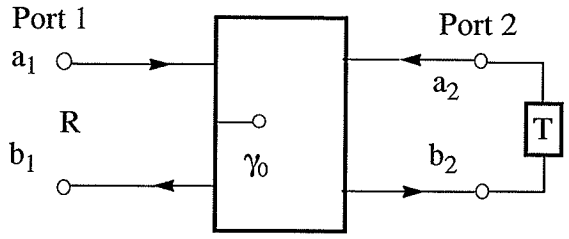

Fig. 2.4 Adaptor representation of an allpass section of degree one.

Proof: First, consider the interconnection of two two-ports, with port resistances R_1 and R_2 (see Figure. 2.5). The wave quantities are related to the voltages and currents by

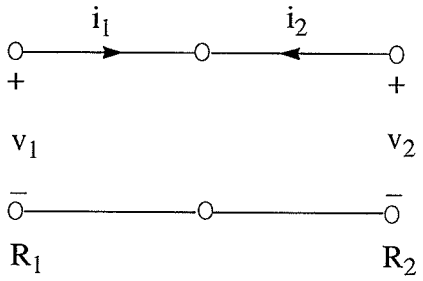

Fig. 2.5 Direct connection of two two-ports.

$$a_1 = v_1 + R_1 i_1 \tag{2.14a}$$

$$b_1 = v_1 - R_1 i_1 \tag{2.14b}$$

$$a_2 = v_2 + R_2 i_2 \tag{2.14c}$$

$$b_2 = v_2 - R_2 i_2 \tag{2.14d}$$

Since the two ports are simply connected, we have

$$v_1 = v_2 \tag{2.15a}$$

$$i_1 = -i_2 \tag{2.15b}$$

Substituting (2.15a) and (2.15b) into (2.14c), we get

$$a_2 = v_1 - R_2 i_1 \tag{2.16}$$

From (2.14a) and (2.16), we get

$$i_1 = -\frac{a_2 - a_1}{R_1 + R_2} \tag{2.17a}$$

$$v_1 = \frac{R_2 a_1 + R_1 a_2}{R_1 + R_2} \tag{2.17b}$$

Substituting (2.17a) and (2.17b) into (2.14b), we get

$$b_1 = a_2 + \gamma_0 (a_2 - a_1) \tag{2.18a}$$

and substituting (2.17a) and (2.17b) into (2.14d), we get

$$b_2 = a_1 + \gamma_0 (a_2 - a_1) \tag{2.18b}$$

where

$$\gamma_0 = \frac{R_1 - R_2}{R_1 + R_2} \tag{2.18c}$$

Also from Figure 2.4, we have $a_2 = z^{-1} b_2$ (2.19)

Substituting (2.19) into (2.18a) and (2.18b)

$$b_1 = (1 + \gamma_0) z^{-1} b_2 - \gamma_0 a_1 \tag{2.20a}$$

$$b_2 = \gamma_0 z^{-1} b_2 + (1 - \gamma_0) a_1 \tag{2.20b}$$

From (2.20b) we get

$$b_2 = \frac{1 - \gamma_0}{1 - \gamma_0 z^{-1}} a_1 \tag{2.21}$$

Substituting (2.21) into (2.20a)

$$S = \frac{b_1}{a_1} = \frac{z^{-1} - \gamma_0}{1 - \gamma_0 z^{-1}} \tag{2.22}$$

Substituting (2.7a) into (2.12)

$$S = \frac{-\frac{z-1}{z+1} + B_0}{\frac{z-1}{z+1} + B_0} = \frac{z^{-1} - \frac{1 - B_0}{1 + B_0}}{1 - \frac{1 - B_0}{1 + B_0} z^{-1}} \tag{2.23}$$

Comparing (2.22) and (2.23), we get

$$\gamma_0 = \frac{1 - B_0}{1 + B_0} \tag{2.24}$$

This completes the proof.

2.2.2 The determination of the multiplier coefficients of a section of degree two

Each of the $\frac{N-1}{2}$ sections of degree two has (as we shall prove below) a reflectance of the following form:

$$S = \frac{\psi^2 - A_i\psi + B_i}{\psi^2 + A_i\psi + B_i} \tag{2.25}$$

It is known [8] that the corresponding wave digital realization has equivalent wave-flow diagrams as in Figure 2.6, where the coefficients are given by

$$\gamma_{2i-1} = \frac{A_i - B_i - 1}{A_i + B_i + 1} \tag{2.26a}$$

and

$$\gamma_{2i} = \frac{1 - B_i}{1 + B_i} \tag{2.26b}$$

where $i = 1, 2, \ldots, \frac{N-1}{2}$

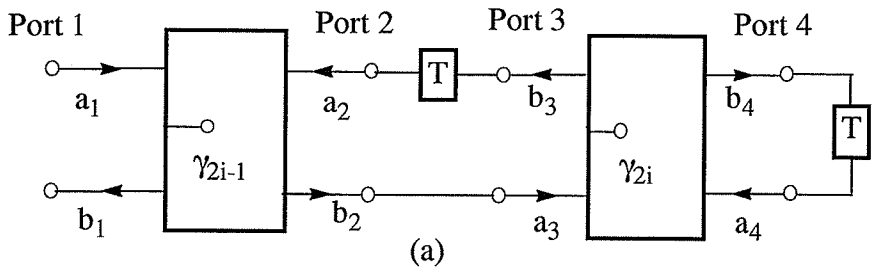

(a)

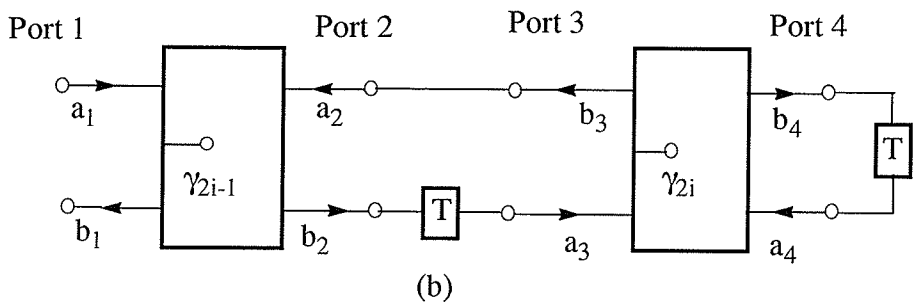

(b)

Fig. 2.6(a), (b) Equivalent wave-flow diagrams of the ith second-degree allpass section.

Proof: first, as in the degree-one case, we have

$$b_1 = a_2 + \gamma_{2i-1}(a_2 - a_1) \qquad (2.27a)$$

$$b_2 = a_1 + \gamma_{2i-1}(a_2 - a_1) \qquad (2.27b)$$

$$b_3 = a_4 + \gamma_{2i}(a_4 - a_3) \qquad (2.27c)$$

$$b_4 = a_3 + \gamma_{2i}(a_4 - a_3) \qquad (2.27d)$$

Also from Figure 2.6(a), we have

$$a_2 = z^{-1} b_3 \qquad (2.28a)$$

$$a_3 = b_2 \qquad (2.28b)$$

$$a_4 = z^{-1} b_4 \qquad (2.28c)$$

Substituting(2.28c) into (2.27d)

$$b_4 = \frac{1 - \gamma_{2i}}{1 - \gamma_{2i} z^{-1}} a_3 \qquad (2.29)$$

Substituting(2.28c), (2.29) and (2.28b) into (2.27c)

$$b_3 = (1 + \gamma_{2i}) z^{-1} \left(\frac{1 - \gamma_{2i}}{1 - \gamma_{2i} z^{-1}} \right) a_3 - \gamma_{2i} a_3$$

$$= \left[\frac{\left(1-\gamma_{2i}{}^{2}\right)z^{-1}}{1-\gamma_{2i}z^{-1}} - \gamma_{2i} \right] a_3$$

$$= \frac{z^{-1}-\gamma_{2i}}{1-\gamma_{2i}z^{-1}} b_2 \qquad (2.30)$$

Substituting(2.30) into (2.28a)

$$a_2 = z^{-1}\left(\frac{z^{-1}-\gamma_{2i}}{1-\gamma_{2i}z^{-1}} \right) b_2 \qquad (2.31)$$

Substituting(2.31) into (2.27b)

$$a_2 = \frac{(1-\gamma_{2i-1})z^{-1} + \gamma_{2i}\gamma_{2i-1} - \gamma_{2i}}{z + \gamma_{2i}\gamma_{2i-1} - \gamma_{2i} - \gamma_{2i-1}z^{-1}} a_1 \qquad (2.32)$$

Substituting(2.32) into (2.27a)

$$S = \frac{b_1}{a_1} = \frac{-\gamma_{2i-1} + \gamma_{2i}(\gamma_{2i-1}-1)z^{-1} + z^{-2}}{1 + \gamma_{2i}(\gamma_{2i-1}-1)z^{-1} - \gamma_{2i-1}z^{-2}} \qquad (2.33)$$

Also, substituting (2.7a) into (2.25)

$$S = \frac{\left(\frac{z-1}{z+1}\right)^2 - A_i\left(\frac{z-1}{z+1}\right) + B_i}{\left(\frac{z-1}{z+1}\right)^2 + A_i\left(\frac{z-1}{z+1}\right) + B_i}$$

$$= \frac{(1-A_i+B_i)z^2 + (2B_i-2)z + (1+A_i+B_i)}{(1+A_i+B_i)z^2 + (2B_i-2)z + (1-A_i+B_i)}$$

$$= \frac{-\frac{A_i-B_i-1}{A_i+B_i+1} + \frac{2(B_i-1)}{A_i+B_i+1}z^{-1} + z^{-2}}{1 + \frac{2(B_i-1)}{A_i+B_i+1}z^{-1} - \frac{A_i-B_i-1}{A_i+B_i+1}z^{-2}} \qquad (2.34)$$

Comparing(2.33) and (2.34), we get

$$\gamma_{2i-1} = \frac{A_i - B_i - 1}{A_i + B_i + 1} \tag{2.35}$$

and

$$\gamma_{2i}(\gamma_{2i-1} - 1) = \frac{2(B_i - 1)}{A_i + B_i + 1} \tag{2.36}$$

Substituting (2.35) into (2.36), we have

$$\gamma_{2i} = \frac{1 - B_i}{1 + B_i} \tag{2.37}$$

This completes the proof.

2.2.3 Synthesis using cascaded allpass functions

We now discuss direct design methods for lattice WDF realizations of the classical filters using the first- and second-degree allpass sections.

Consider one of the Butterworth, Chebyshev or Cauer parameter (elliptic) reference filters. Let $g(\psi)$ be given in the product form

$$g(\psi) = (\psi + B_0) \prod_{i=1}^{(N-1)/2} \left(\psi^2 + \psi A_i + B_i\right) \tag{2.38}$$

From this, $g_1(\psi)$ and $g_2(\psi)$ can be obtained using the alternating property relating to the distribution of the their zeros. Thus the allpass functions S_1 and S_2 can be written as the following product of sections of degree one and two.

$$S_1(\psi) = \frac{-\psi + B_0}{\psi + B_0} \cdot \frac{\psi^2 - \psi A_2 + B_2}{\psi^2 + \psi A_2 + B_2} \cdot \frac{\psi^2 - \psi A_4 + B_4}{\psi^2 + \psi A_4 + B_4} \cdot \ldots \cdot \frac{\psi^2 - \psi A_k + B_k}{\psi^2 + \psi A_k + B_k}$$

$$S_2(\psi) = \frac{\psi^2 - \psi A_1 + B_1}{\psi^2 + \psi A_1 + B_1} \cdot \frac{\psi^2 - \psi A_3 + B_3}{\psi^2 + \psi A_3 + B_3} \cdot \ldots \cdot \frac{\psi^2 - \psi A_l + B_l}{\psi^2 + \psi A_l + B_l}$$

where

$$k = \frac{N-1}{2},\ l = \frac{N-3}{2}, \text{ or } k = \frac{N-3}{2},\ l = \frac{N-1}{2}.$$

All adaptor coefficients can be computed by (2.13) and (2.26). Using the cascade synthesis of these elementary sections, realizations of S_1 and S_2 are obtained, which leads to the corresponding block diagram for the filter given in Figure 2.7.

In the most common cases, i.e., for Butterworth, Chebyshev and Cauer (elliptic) reference filters, A_i, B_i of (2.38) can be obtained by the formulas given in [8] and [19]. So the construction of explicit formulas for the above structure of a WDF is availible [8]. We note that all these filters are odd order and have real coefficients.

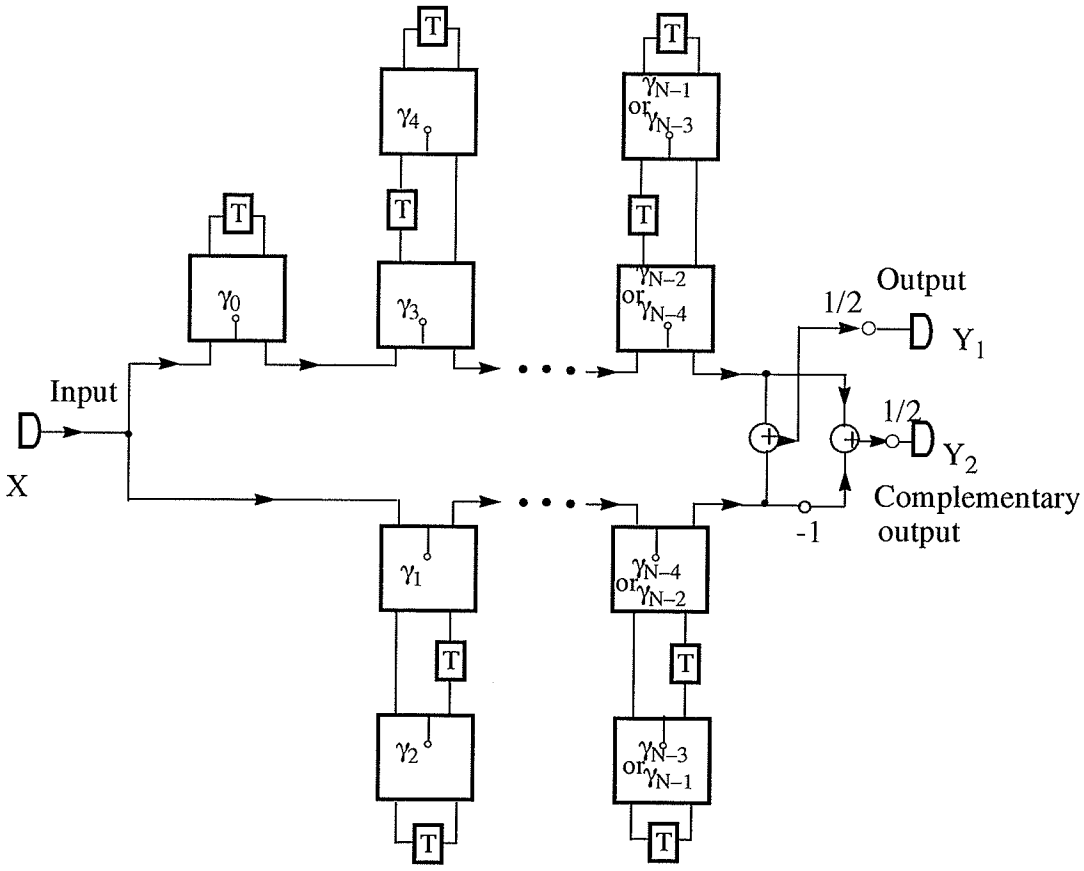

Fig.2.7. Block diagram of the lattice WDF with cascaded allpass sections for N = 5, 9, 13, ... (as the top structure), or N = 7, 11, 15, ...(as the bottom structure).

Chapter 3

A direct design method for complex WDF

This chapter presents complex wave digital filter (CWDF) realizations of even-order classical reference filters. We discuss how to decompose an even-order transfer function in the z-variable into a sum of two complex allpass functions in Section 3.1. The corresponding CWDF theory is given in Section 3.2. Section 3.3 gives a realization of a degree-one allpass section by a two-port adaptor with a delay. Section 3.4 describes transformations between the variables. Section 3.5 presents synthesis using cascaded allpass sections. Finally in Section 3.6, a process to optimize the wordlength of the cross adaptor coefficients is described.

3.1 Decomposition of an even-order lowpass transfer function

In this section, we discuss decomposing a general even-order digital filter transfer function $G(z)$ in the z-domain into the sum of complex allpass functions. The method was introduced in [9] and we will show how this idea can be used to implement even-order filters.

Consider a stable transfer function $G(z)$ that is real-valued for real z and satisfies

$\left|G\left(e^{j\omega}\right)\right| \leq 1$, for all real ω, where $z = e^{j\omega}$. Such transfer functions are said to be bounded real. There exists a certain class of bounded real transfer functions (including the classical filters discussed in Chapter 2) that can be implemented in the form of a parallel interconnection of two allpass filters $A_1(z)$, $A_2(z)$ (Figure 3.1) [9] with real coefficients. This observation was first made in connection with wave digital filters [15]. The allpass functions can be implemented as a cascade of lossless lattice structures (see Chapter 2). The key point concerning the implementation as a sum of two allpass sections is that each allpass function can be implemented as a cascade of first-degree allpass sections.

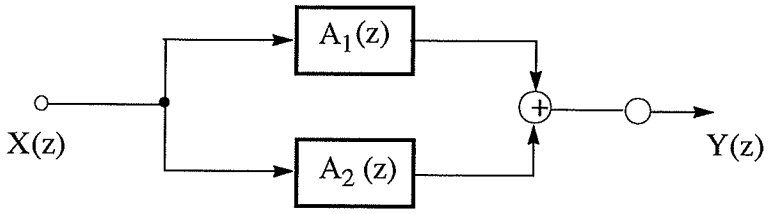

Fig. 3.1 Parallel connection of two allpass sections.

There are certain conditions that a bounded real transfer function $G(z)$ has to satisfy in order to be implemented as in Figure 3.1. In particular, let $G(z)$ be an Nth-order lowpass transfer function of the form

$$G(z) = \frac{P(z)}{D(z)} \tag{3.1a}$$

where

$$P(z) = p_0 + p_1 z^{-1} + \ldots + p_N z^{-N} \tag{3.1b}$$

$$D(z) = 1 + d_1 z^{-1} + \ldots + d_N z^{-N} \tag{3.1c}$$

Here, p_n, d_n $(n = 0, 1, 2, \ldots, N)$ are real and $P(z)$ is a symmetric polynomial, i.e.,

$$P\left(z^{-1}\right) = z^{N} P(z) \tag{3.2}$$

It can be shown that N has to be odd so that an implementation in the form of Figure 3.1 is feasible [9]. For example, odd-order --but not even-order-- lowpass Butterworth, Chebyshev, and Cauer filters can be implemented as in Figure 3.1 (the corresponding lattice WDFs diagram was given in Figure 2.2).

So for even N, an implementation in the form of Figure 3.1 is impossible. Here, we describe a modification given in [14] for the case of an even-order lowpass function $G(z)$. Specifically, we decompose $G(z)$ into a sum of allpass functions $A_1(z)$ and $A_2(z)$ with complex coefficients [9].

Consider an Nth-order bounded real function $G(z) = P(z)/D(z)$ as in (3.1) given in minimal form (i.e., no common factors between $P(z)$ and $D(z)$). Assume that $P(z)$ is a symmetric polynomial satisfying (3.2). Let $H(z)$ be a bounded real function with the same denominator $D(z)$. Then

$$H(z) = \frac{Q(z)}{D(z)} = \frac{q_0 + q_1 z^{-1} + \ldots q_N z^{-N}}{1 + d_1 z^{-1} + \ldots d_N z^{-N}} \tag{3.3}$$

such that $\{G(z), H(z)\}$ are a power-complementary pair, i.e., satisfy

$$\left|G\left(e^{j\omega}\right)\right|^2 + \left|H\left(e^{j\omega}\right)\right|^2 = 1 \tag{3.4}$$

Such an $H(z)$ can always be constructed by finding a spectral factor $Q\left(e^{j\omega}\right)$ of the positive function $\left(\left|D\left(e^{j\omega}\right)\right|^2 - \left|P\left(e^{j\omega}\right)\right|^2\right)$. In many filtering applications, it is possible to

find a spectral factor $Q(z)$ such that $Q(z)$ is symmetric.

So assume that $P(z)$ and $Q(z)$ are both symmetric. We know that, by analytic continuation, (3.4) implies

$$\tilde{G}(z)G(z) + \tilde{H}(z)H(z) = 1 \qquad (3.5)$$

except at the poles, where $\tilde{G}(z)$ and $\tilde{H}(z)$ are the functions obtained from $G(z)$ and $H(z)$ by replacing z by z^{-1} and all complex coefficients are conjugated. Also, from (3.1a) and (3.3) this implies

$$\tilde{P}(z)P(z) + \tilde{Q}(z)Q(z) = \tilde{D}(z)D(z) \qquad (3.6)$$

Since $P(z)$ and $Q(z)$ are symmetric, we can write

$$\tilde{P}(z) = z^{N}P(z) \qquad \tilde{Q}(z) = z^{N}Q(z) \qquad (3.7)$$

Then (3.6) becomes

$$P^{2}(z) + Q^{2}(z) = z^{-N}D\left(z^{-1}\right)D(z) \qquad (3.8)$$

which can be decomposed as

$$[P(z) + jQ(z)]\,[P(z) - jQ(z)] = z^{-N}D\left(z^{-1}\right)D(z) \qquad (3.9)$$

Let $\{z_1, z_2, \ldots, z_n\}$ denote the zeros of $D(z)$. None of them can be real for the following reason: If z_r were a real zero of $D(z)$, then it would certainly be a zero of $P(z) + jQ(z)$ or $P(z) - jQ(z)$. Assume for example, that $P(z_r) + jQ(z_r) = 0$. Since z_r is real and $P(z)$ has real cofficients, $P(z_r)$ is real, and so is $Q(z_r)$. Accordingly, we must have $P(z_r) = Q(z_r) = 0$. In particular, this implies a common factor $\left(1 - z^{-1}z_r\right)$

between $P(z)$ and $D(z)$, which has been ruled out earlier.

All the above z_k's occur in complex conjugate pairs (since $D(z)$ is a polynomial with real coefficients). Hence

$$D(z) = \prod_{k=1}^{M} \left(1 - z^{-1} z_k\right)\left(1 - z^{-1} z_k^*\right), \qquad M = \frac{N}{2} \tag{3.10}$$

As a result, (3.9) can be rewritten as

$$[P(z) + jQ(z)]\,[P(z) - jQ(z)]$$

$$= z^{-N} \prod_{k=1}^{M} \left(1 - z^{-1} z_k\right)\left(1 - z^{-1} z_k^*\right)(1 - z z_k)\,(1 - z z_k^*) \tag{3.11}$$

Since $P(z)$ and $Q(z)$ are symmetric polynomials with real coefficients, the zeros of $P(z) + jQ(z)$ occur in reciprocal pairs, as do the zeros of $P(z) - jQ(z)$. Moreover, if z_k is a zero of $P(z) + jQ(z)$, then its conjugate z_k^* is a zero of $P(z) - jQ(z)$. In conclusion, the zeros shown on the right-hand side of (3.11) can be assigned as follows:

$$P(z) + jQ(z) = \lambda z^{-M} \prod_{k=1}^{M} \left(1 - z^{-1} z_k\right)(1 - z z_k) \tag{3.12}$$

$$P(z) - jQ(z) = \lambda^* z^{-M} \prod_{k=1}^{M} \left(1 - z^{-1} z_k^*\right)(1 - z z_k^*) \tag{3.13}$$

where λ is a complex unimodular constant. Dividing both sides of (3.12) and (3.13) by $D(z)$ in (3.10), we get

$$G(z) + jH(z) = \lambda \prod_{k=1}^{M} \frac{z^{-1} - z_k}{1 - z^{-1} z_k^*} \tag{3.14}$$

$$G(z) - jH(z) = \lambda^* \prod_{k=1}^{M} \frac{z^{-1} - z_k^*}{1 - z^{-1} z_k} \tag{3.15}$$

Thus, $G(z)$ and $H(z)$ can be written as linear combinations of stable allpass functions

$$G(z) = \frac{1}{2}[A_1(z) + A_2(z)] \tag{3.16}$$

$$H(z) = \frac{1}{2j}[A_1(z) - A_2(z)] \tag{3.17}$$

where

$$A_1(z) = \lambda \prod_{k=1}^{M} \frac{z^{-1} - z_k}{1 - z^{-1} z_k^*} \tag{3.18}$$

$$A_2(z) = \lambda^* \prod_{k=1}^{M} \frac{z^{-1} - z_k^*}{1 - z^{-1} z_k} \tag{3.19}$$

Note that $A_1(z)$ and $A_2(z)$ have complex coefficients, and the coefficients of $A_2(z)$ are the conjugates of the coefficients of $A_1(z)$. Figure 3.2 represents the allpass decomposition scheme.

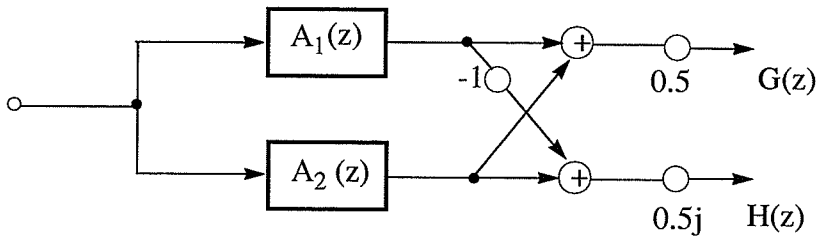

Fig. 3.2 Implementing the allpass complementary pair.

Also, since the coefficients of $A_2(z)$ are complex conjugates of those in $A_1(z)$, it is

only required to implement $A_1(z)$ if the input is real. The real part of the filtered output sequence is the output corresponding to $G(z)$, while the imaginary part of the output sequence of $A_1(z)$ is the output corresponding to $H(z)$ as in Figure 3.3.

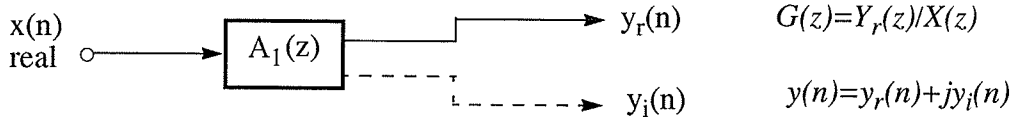

Fig. 3.3. Implementation of $G(z)$ by means of a single complex allpass function.

In summary, given any bounded real function $G(z) = P(z)/D(z)$ with symmetric numerator $P(z)$, we can always obtain the implementation of Figure 3.1 or Figure 3.2 if there exists a bounded real function $H(z) = Q(z)/D(z)$ with symmetric numerator $Q(z)$, such that (3.5), (or equivalently (3.6)) holds. The above-mentioned conditions on $G(z)$ and $H(z)$ can be found in a class of selective filters. For example, even-ordered Butterworth, Chebyshev and Cauer digital transfer functions satisfy the above requirements.

3.2 The corresponding classical complex wave digital theory

In this section, we present a decomposition similar to that of Section 3.1 and similar to that in [5] using wave digital theory. Therefore, the discussion will be in the ψ -domain.

In Section 2.1, we have discussed the classical wave digital theory and the scattering equation. For a complex wave digital network, there is similarly a scattering equation and

the scattering matrix given by [24], [23] as follows.

$$\begin{bmatrix} B_1 \\ B_2 \end{bmatrix} = S \begin{bmatrix} A_1 \\ A_2 \end{bmatrix} \tag{3.20}$$

with the scattering matrix

$$S = \frac{1}{g} \begin{bmatrix} h & \sigma f_* \\ f & -\sigma h_* \end{bmatrix} . \tag{3.21}$$

The polynomials f, g, h satisfy the following conditions:

(1) $f = f(\psi)$, $g = g(\psi)$, $h = h(\psi)$ are real or complex polynomials (i.e. real or complex coefficients) in the complex frequency variable ψ. The subscript asterisk denotes paraconjugation, i.e., $f_*(\psi) \equiv f^*(-\psi^*)$ where the superscript asterisk designates complex conjugate. For a real polynomial $f_*(\psi) = f(-\psi)$

(2) $g(\psi)$ is a Hurwitz polynomial.

(3) f, g, and h are related by

$$g g_* = h h_* + f f_* \tag{3.22}$$

(4) σ is a constant with $|\sigma| = 1$, therefore for a real constant either $\sigma = 1$ or $\sigma = -1$.

For real polynomials f, g, and h, we know that in the reciprocal case:

$$f = \sigma f_* \qquad (\text{i.e. } s_{12} = s_{21}) \tag{3.23}$$

and in the antimetric (antisymmetric) case:

$$h = \sigma h_* \qquad (\text{i.e. } s_{22} = -s_{11}) \tag{3.24}$$

Under the conditions (3.23) and (3.24), (3.21) becomes

$$S = \frac{1}{g}\begin{bmatrix} h & f \\ f & -h \end{bmatrix} \tag{3.25}$$

and (3.22) becomes

$$h^2 + f^2 = \sigma g g_* \tag{3.26}$$

For the real case $g_*(\psi) = g(-\psi)$; let us consider:

$$\psi = 0 : g_*(0) = g(0) \tag{3.27}$$

Then from (3.26), we have

$$h^2(0) + f^2(0) = \sigma g(0) g_*(0) = \sigma g^2(0) \tag{3.28}$$

which shows $\sigma = 1$.

Let the degree of g be n, and its highest coefficient be g_n, then

$$g_{*_n} = (-1)^n g_n \tag{3.29}$$

Since the highest coefficient of $h^2 + f^2$ must be positive, the highest coeficient of gg_* must be positive. Then we get

$$0 < g_n g_{*_n} = (-1)^n g_n g_n = (-1)^n g_n^2 \tag{3.30}$$

and thus, n must be even.

Also, with $\sigma = 1$, (3.23) becomes $f = f_*$, (3.24) becomes $h = h_*$. Therefore f and h must have even degree.

Thus we have

$$h^2 + f^2 = (h + jf)(h - jf) = gg_* \qquad (3.31)$$

which will be required for the decomposition derived below. We can assume without loss of generality that f and g are relatively prime, then g can not have real zeros; because if $gg_* = 0$ for ψ_0 real, then $h(\psi_0)$ and $f(\psi_0)$ are real and both must be zero from (3.31), i.e. $h(\psi_0) = 0$ and $f(\psi_0) = 0$, which implies f and h have a common zero which has been ruled out. (Note that a similar proof of the corresponding result in the z-domain was given in Section 3.1.) Thus g cannot have real zeros and the zeros of (3.31) must appear with quadrantal symmetry (gg_* is an even polynomial). Without loss of generality assume f is monic. Let

$$g(\psi) = k\prod_{i=1}^{n/2} (\psi - \psi_i)(\psi - \psi_i^*) \qquad (3.32)$$

where $Re\{\psi_i\} < 0$ and k is real.

Substituting (3.32) into (3.31)

$$h^2(\psi) + f^2(\psi) = (f(\psi) + jh(\psi))(f(\psi) - jh(\psi))$$

$$= g(\psi) g_*(\psi)$$

$$= k^2 \prod_{i=1}^{n/2} (\psi - \psi_i)(\psi - \psi_i^*)(\psi + \psi_i)(\psi + \psi_i^*) \qquad (3.33)$$

Let

$$v(\psi) = ke^{j\theta} \prod_{i=1}^{n/2} (\psi + \psi_i^*)(\psi - \psi_i^*) \qquad (3.34a)$$

then

$$v_*(\psi) = ke^{-j\theta}\prod_{i=1}^{n/2}(\psi+\psi_i)(\psi-\psi_i) \tag{3.34b}$$

and

$$v(\psi)\,v_*(\psi) = g(\psi)\,g_*(\psi) \tag{3.35}$$

We can identify $f(\psi)+jh(\psi)$ with $v(\psi)$ and $f(\psi)-jh(\psi)$ with $v_*(\psi)$. The factor $e^{j\theta}$ remains to be determined from a given f and g.

$$f(\psi) = \frac{1}{2}(v(\psi)+v_*(\psi))$$

$$= \frac{k}{2}\left(e^{j\theta}\prod_{i=1}^{n/2}(\psi+\psi_i^*)(\psi-\psi_i^*) + e^{-j\theta}\prod_{i=1}^{n/2}(\psi+\psi_i)(\psi-\psi_i)\right) \tag{3.36}$$

$$h(\psi) = \frac{1}{2j}(v(\psi)-v_*(\psi))$$

$$= \frac{k}{2j}\left(e^{j\theta}\prod_{i=1}^{n/2}(\psi+\psi_i^*)(\psi-\psi_i^*) - e^{-j\theta}\prod_{i=1}^{n/2}(\psi+\psi_i)(\psi-\psi_i)\right) \tag{3.37}$$

Dividing both side of (3.36) and (3.37) by $g(\psi)$ in (3.32)

$$\frac{f(\psi)}{g(\psi)} = \frac{1}{2}\left(e^{j\theta}\prod_{i=1}^{n/2}\frac{\psi+\psi_i^*}{\psi-\psi_i} + e^{-j\theta}\prod_{i=1}^{n/2}\frac{\psi+\psi_i}{\psi-\psi_i^*}\right) \tag{3.38a}$$

$$\frac{h(\psi)}{g(\psi)} = \frac{1}{2j}\left(e^{j\theta}\prod_{i=1}^{n/2}\frac{\psi+\psi_i^*}{\psi-\psi_i} - e^{-j\theta}\prod_{i=1}^{n/2}\frac{\psi+\psi_i}{\psi-\psi_i^*}\right) \tag{3.38b}$$

Let

$$A_1(\psi) = e^{j\theta}\prod_{i=1}^{n/2}\frac{\psi+\psi_i^*}{\psi-\psi_i} \tag{3.39a}$$

$$A_2(\psi) = e^{-j\theta}\prod_{i=1}^{n/2}\frac{\psi+\psi_i}{\psi-\psi_i^*} \tag{3.39b}$$

Then we can write

$$\frac{f(\psi)}{g(\psi)} = \frac{1}{2}(A_1(\psi)+A_2(\psi)) \tag{3.40a}$$

$$\frac{h(\psi)}{g(\psi)} = \frac{1}{2j}(A_1(\psi)-A_2(\psi)) \tag{3.40b}$$

To complete the determination of $A_1(\psi)$ and $A_2(\psi)$ from $f(\psi)$ and $g(\psi)$, $e^{j\theta}$ is evaluated from

$$\frac{f}{g}(\infty) = \frac{1}{2}\left(e^{j\theta}+e^{-j\theta}\right) = \cos\theta \tag{3.41a}$$

$$\frac{h}{g}(\infty) = \frac{1}{2j}\left(e^{j\theta}-e^{-j\theta}\right) = \sin\theta \tag{3.41b}$$

If h is unknown, we can calculate $\frac{f}{g}(\infty)$ and $\frac{f}{g}(0)$ to evaluate $e^{j\theta}$.

Also, corresponding to the odd case, the poles of even-order $A_1(\psi)$ and $A_2(\psi)$ are alternately distributed in a cyclic manner[12] (see Figure 3.4). Again, this property will be used to determine $A_1(\psi)$.

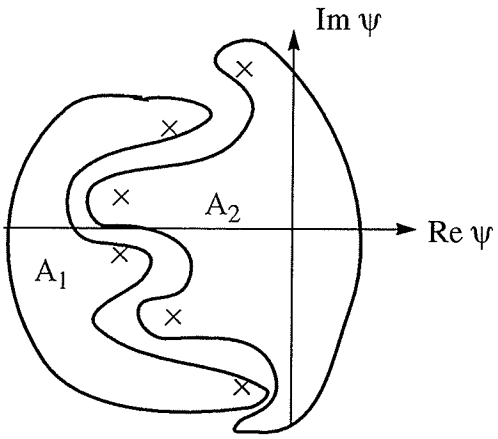

Fig. 3.4 Alternating distribution of the poles of the polynomial A_1 and A_2.

3.3 Realizations of complex sections of degree one

To implement (3.40), we need to realize complex sections of degree one $S(\psi) = \dfrac{\psi + \psi_k^*}{\psi - \psi_k}$. In the z-variable, a complex allpass section of degree one has a reflectance of the following form:

$$S = \frac{z^{-1} - z_k}{1 - z_k^* z^{-1}} \tag{3.42}$$

In [3], Scarth and Martens gave a realization of a complex WDF through an extraction process with complex two-port adaptors and delays. Here we present a realization using a complex two-port and a delay. Let us consider a complex two-port adaptor as in Figure 3.5.

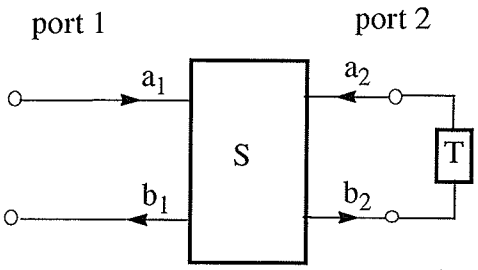

Fig. 3.5 A complex all-pass section of degree one.

Let

$$\boldsymbol{S} = \frac{1}{g}\begin{bmatrix} h & \sigma f_* \\ f & -\sigma h_* \end{bmatrix} \tag{3.43}$$

be the scattering matrix where f, g, h are complex constants that satisfy the conditions (3.22) in Section 3.2. Since g is a scaling constant, let $g = 1$. Then

$$\boldsymbol{S} = \begin{bmatrix} h & \sigma f_* \\ f & -\sigma h_* \end{bmatrix} \quad \text{and} \quad |f|^2 + |h|^2 = 1. \tag{3.44}$$

From the scattering equation and the diagram, we obtain

$$b_1 = ha_1 + \sigma f^* a_2 \tag{3.45a}$$

$$b_2 = fa_1 - \sigma h^* a_2 \tag{3.45b}$$

$$a_2 = z^{-1} b_2 \tag{3.46}$$

Substituting (3.46) into (3.45b), we have

$$a_2 = \frac{f}{z + \sigma h^*} a_1 \tag{3.47}$$

Substituting (3.47) into (3.45a), we have

$$\frac{b_1}{a_1} = h + \frac{\sigma f f^*}{z + \sigma h^*} = \frac{h + \sigma (h h^* + f f^*) z^{-1}}{1 + \sigma h^* z^{-1}} \tag{3.48}$$

$$= \sigma \frac{z^{-1} + \dfrac{h}{\sigma}}{1 + \sigma h^* z^{-1}} = \sigma \frac{z^{-1} + \sigma^* h}{1 + \sigma h^* z^{-1}} \tag{3.49}$$

This is in the form (3.42). Let

$$\frac{h}{\sigma} = -z_k, \quad \text{i.e.} \quad h = -\sigma z_k \tag{3.50}$$

Write z_k, σ in polar form, i.e. $z_k = re^{j\phi}$, $\sigma = e^{j\theta_1}$ to obtain

$$|f|^2 = 1 - |h|^2 = 1 - r^2 \text{ , i.e. } |f| = \sqrt{1 - r^2}, f = \sqrt{1 - r^2} e^{j\theta_2}.$$

So

$$\boldsymbol{S} = \begin{bmatrix} -re^{j(\phi + \theta_1)} & \sqrt{1 - r^2} e^{-j(\theta_2 - \theta_1)} \\ \sqrt{1 - r^2} e^{j\theta_2} & re^{-j\phi} \end{bmatrix} \tag{3.51}$$

Here, we consider two cases: first, $\theta_1 = 0$, $\theta_2 = 0$; and second, $\theta_1 = -\phi$, $\theta_2 = \theta_1$.

3.3.1 Complex wave digital cross adaptor

If $\theta_1 = 0$, $\theta_2 = 0$, then

$$\boldsymbol{S} = \begin{bmatrix} -re^{j\phi} & \sqrt{1 - r^2} \\ \sqrt{1 - r^2} & re^{-j\phi} \end{bmatrix} \tag{3.52}$$

We can scale $\boldsymbol{S}$ by introducing the transformation

$$\boldsymbol{DSD}^{-1} = \begin{bmatrix} 1 & 0 \\ 0 & d_2 \end{bmatrix} \begin{bmatrix} -re^{j\phi} & \sqrt{1 - r^2} \\ \sqrt{1 - r^2} & re^{-j\phi} \end{bmatrix} \begin{bmatrix} 1 & 0 \\ 0 & \dfrac{1}{d_2} \end{bmatrix} = \begin{bmatrix} -re^{j\phi} & \dfrac{1}{d_2}\sqrt{1 - r^2} \\ d_2\sqrt{1 - r^2} & re^{-j\phi} \end{bmatrix} \tag{3.53}$$

where $\boldsymbol{D} = \begin{bmatrix} 1 & 0 \\ 0 & d_2 \end{bmatrix}$, $\boldsymbol{D}^{-1} = \begin{bmatrix} 1 & 0 \\ 0 & \frac{1}{d_2} \end{bmatrix}$.

Let $d_2 = \sqrt{1 - r^2}$, then

$$\boldsymbol{DSD}^{-1} = \begin{bmatrix} -re^{j\phi} & 1 \\ 1 - r^2 & re^{-j\phi} \end{bmatrix} \tag{3.54}$$

We note that the scattering matrix (3.54) is the same form as the complex cross adaptor scattering matrix [10] if we let $\beta = -re^{j\phi}$. The complex cross adaptor signal-flow diagram is as shown in Figure 3.6(a). Expressing b_1 and b_2 as functions of a_1 and a_2, we obtain

$$b_1 = \beta a_1 + a_2 \tag{3.55a}$$

$$b_2 = -\beta^* b_1 + a_1 \tag{3.55b}$$

We can also write the relationship as

$$b_1 = \beta a_1 + a_2 \tag{3.56a}$$

$$b_2 = \left(1 - |\beta|^2\right) a_1 - \beta^* a_2 \tag{3.56b}$$

The symbolic representation is given in Figure 3.6b. For the realization of CWDFs, this complex cross adaptor offers several advantages. The two constants β and $-\beta^*$ differ from each other only in the sign of their real parts and must have a magnitude less than unity. So essentially, there is only one coefficient involved. A physical interpretation of the complex cross adaptor is given by Martens [6] using the relationship between the hybrid

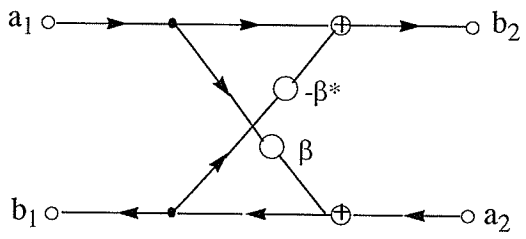

(a)

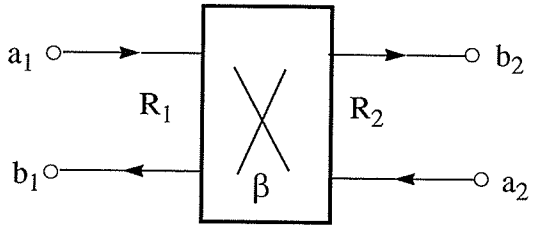

(b)

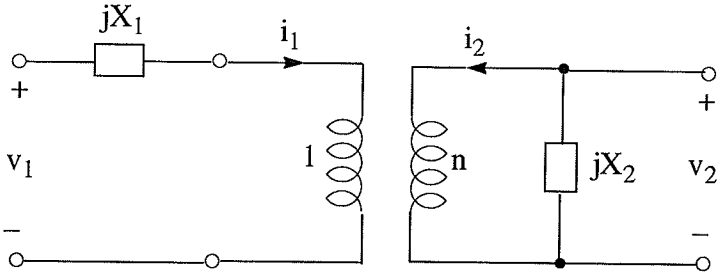

(c)

Fig.3.6.(a) Signal-flow diagram of complex cross adaptor.

(b) Symbolic representation of (a).

(c) Physical interpretation of (a).

matrix and the scattering matrix as shown in Figure 3.6(c), where $X_1 = \dfrac{Im\{\beta\} R_1}{1 - Re\{\beta\}}$,

$X_2 = \dfrac{R_2 (1 - Re\{\beta\})}{Im\{\beta\}}$, and $n = 1 - Re\{\beta\}$.

The complex cross adaptor can be used to realize a complex allpass section of degree

one. We know that a complex allpass section of degree one has a reflectance of the following form $S = \dfrac{z^{-1} - z_k}{1 - z_k^* z^{-1}}$ and the corresponding signal-flow diagram of a wave digital realization is given in Figure 3.7, where the multiplier coefficient is given by

$$\beta = -z_k \tag{3.57}$$

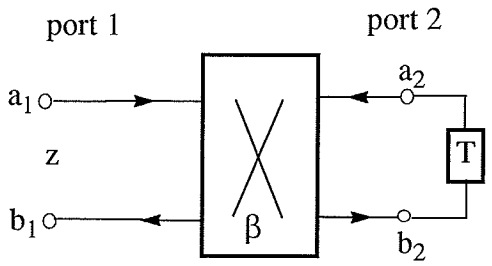

Fig.3.7 Adaptor representation of a complex cross allpass section of degree one.

Here, we check the pseudolosslessness property of the cross adaptor

$$\boldsymbol{S} = \begin{bmatrix} \beta & 1 \\ 1 - |\beta|^2 & -\beta^* \end{bmatrix} \tag{3.58}$$

Comparing (3.54) and (3.58), we have

$$\beta = -re^{j\phi}$$

Let

$$\boldsymbol{G} = (\boldsymbol{D}^{-1})^2 = \begin{bmatrix} 1 & 0 \\ 0 & \dfrac{1}{1 - r^2} \end{bmatrix} = \begin{bmatrix} 1 & 0 \\ 0 & \dfrac{1}{1 - |\beta|^2} \end{bmatrix} \tag{3.59}$$

The condition for pseudolosslessness is given as [3]

$$\boldsymbol{G} = \boldsymbol{S}^{*\mathrm{T}} \boldsymbol{G} \boldsymbol{S} \tag{3.60}$$

To check whether (3.60) is satisfied, we note that

$$\boldsymbol{S}^{*\mathrm{T}}\boldsymbol{G}\boldsymbol{S} = \begin{bmatrix} \beta^* & 1-|\beta|^2 \\ 1 & -\beta \end{bmatrix} \begin{bmatrix} 1 & 0 \\ 0 & \dfrac{1}{1-|\beta|^2} \end{bmatrix} \begin{bmatrix} \beta & 1 \\ 1-|\beta|^2 & -\beta^* \end{bmatrix}$$

$$= 1 \begin{bmatrix} \beta^* & 1 \\ 1 & -\beta\dfrac{1}{1-|\beta|^2} \end{bmatrix} \begin{bmatrix} \beta & 1 \\ 1-|\beta|^2 & -\beta^* \end{bmatrix} = \begin{bmatrix} 1 & 0 \\ 0 & \dfrac{1}{1-|\beta|^2} \end{bmatrix} = \boldsymbol{G}$$

Therefore, the complex cross adaptor structure is pseudolossless as expected.

3.3.2 Complex wave digital adaptor from real wave digital adaptor

If $\theta_1 = -\phi$, $\theta_2 = \theta_1$, then

$$\boldsymbol{S} = \begin{bmatrix} -r & \sqrt{1-r^2} \\ \sqrt{1-r^2}\,e^{-j\phi} & re^{-j\phi} \end{bmatrix} = \begin{bmatrix} 1 & 0 \\ 0 & e^{-j\phi} \end{bmatrix} \begin{bmatrix} -r & \sqrt{1-r^2} \\ \sqrt{1-r^2} & r \end{bmatrix} \tag{3.61}$$

Similarly to the cross adaptor, we use scaling

$$\boldsymbol{D}\boldsymbol{S}\boldsymbol{D}^{-1} = \begin{bmatrix} 1 & 0 \\ 0 & e^{-j\phi} \end{bmatrix} \begin{bmatrix} -r & \dfrac{1}{d_2}\sqrt{1-r^2} \\ d_2\sqrt{1-r^2} & r \end{bmatrix} \tag{3.62}$$

Let $d_2 = \dfrac{\sqrt{1-r^2}}{1+r}$, then

$$\boldsymbol{D}\boldsymbol{S}\boldsymbol{D}^{-1} = \begin{bmatrix} 1 & 0 \\ 0 & e^{-j\phi} \end{bmatrix} \begin{bmatrix} -r & 1+r \\ 1-r & r \end{bmatrix} \tag{3.63}$$

We note that this is the real adaptor scattering matrix with a unimodular multiplier, we have the corresponding wave-flow diagram as shown in Figure 3.8.

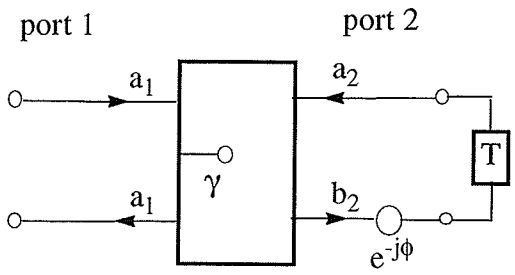

Fig.3.8. A complex two-port adaptor representation with a real two-port adaptor and a unimodular multiplier.

3.4 Transformation from ψ-domain to z-domain

The complex wave digital filter realizations in Section 3.3 are all designed directly in the z-domain for convenience. However, in the classical wave digital theory, transfer functions are usually given in the ψ-domain, and so it is preferred to design the filters in the ψ-domain. All the functions and their relationships in the z-variable described in Section 3.1 can be easily transformed into the ψ-variable by the bilinear transformation $z = \frac{1+\psi}{1-\psi}$ ($\psi = \frac{z-1}{z+1}$). This is a one-to-one transformation that maps the whole of ψ-domain onto the whole of z-domain and vice versa. The imaginary axis in the ψ-domain maps onto the unit circle in the z-domain and the left and right halves of the ψ-domain correspond to the inside and outside of the unit circle in the z-domain, respectively. The point $\psi = 0$ transforms to $z = 1$, and $\psi = \infty$ to $z = -1$.

Consider a complex allpass function of degree one in the ψ-variable

$$C(\psi) = \frac{\psi + \psi_i^*}{\psi - \psi_i} \qquad (3.64)$$

From the definition $\psi = \frac{z-1}{z+1}$, we obtain in the z-plane

$$C(z) = \frac{\frac{1-z^{-1}}{1+z^{-1}} + \psi^*}{\frac{1-z^{-1}}{1+z^{-1}} - \psi} = \frac{(\psi_i^* - 1)z^{-1} + (\psi_i^* + 1)}{-(\psi_i + 1)z^{-1} - (\psi_i - 1)}$$

$$= -\left(\frac{\psi_i^* - 1}{\psi_i - 1}\right)\frac{z^{-1} + \frac{\psi_i^* + 1}{\psi_i^* - 1}}{1 + \frac{\psi_i + 1}{\psi_i - 1}z^{-1}} \tag{3.65}$$

Let

$$\beta = \frac{\psi_i^* + 1}{\psi_i^* - 1} \tag{3.66}$$

Then, we have

$$\psi_i^* = \frac{\beta + 1}{\beta - 1} \tag{3.67}$$

Thus, we get

$$C(z) = \left(-\frac{\beta^* - 1}{\beta - 1}\right)\frac{z^{-1} + \beta}{1 + \beta^* z^{-1}} \tag{3.68}$$

Therefore $C(z)$ can be realized by the implementation of the complex cross adaptor of Section 3.3 and a unimodular multiplier.

3.5 Synthesis using cascaded complex allpass functions

From the realization of real wave digital filter theory [1], [2], a chain connection of allpass sections of degrees 1 and 2 can be obtained by means of three-port circulators ter-

minated at one port by a capacitance or an inductance or by a parallel- or series-resonant circuit. Similarly, a complex chain connection of first-degree allpass sections using three-port circulators and constant reactance networks N_1, N_2, ..., N_n, terminated in a capactance can be used to obtain an n th order allpass as shown in Figure 3.9(a). The constant reactance networks N_1, N_2, ..., N_n are realized by the circuit in Figure 3.6(c).

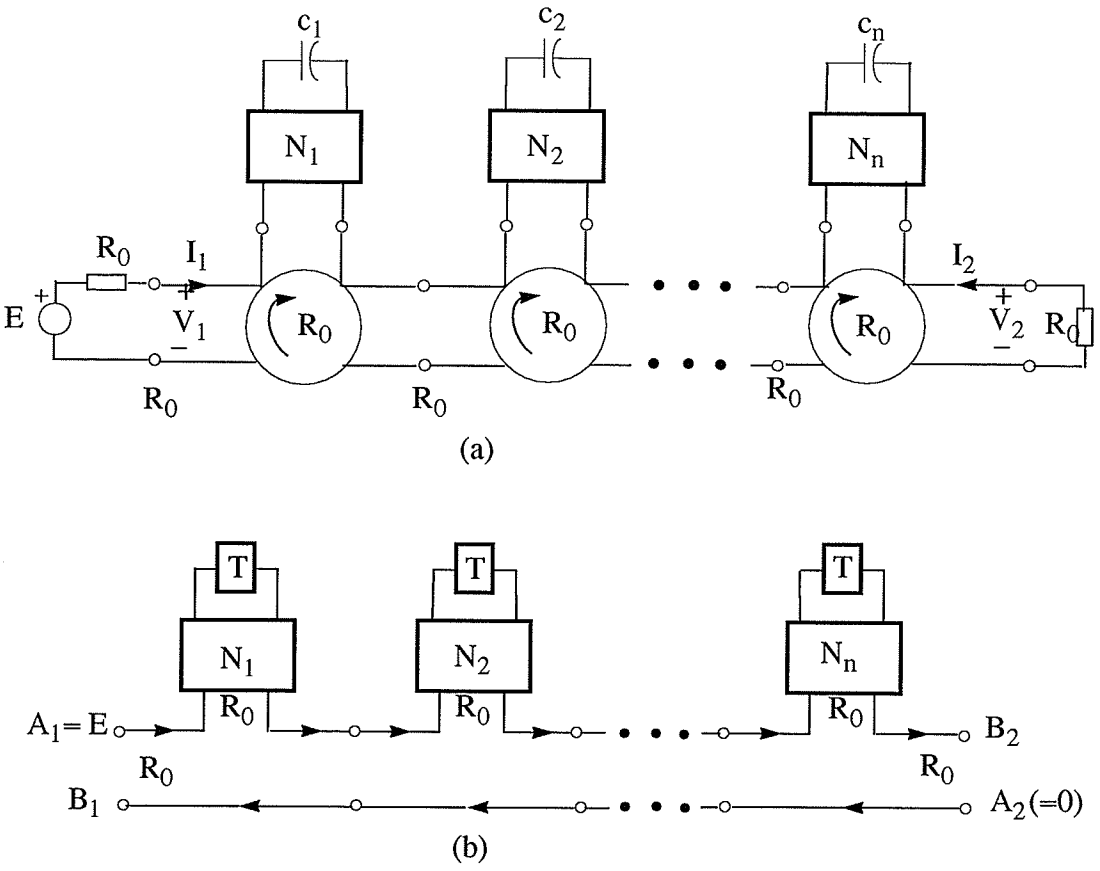

Fig. 3.9. (a) An allpass complex two-port inserted between resistive terminations. (b) General structure of the resulting complex WDF realization, N_1 to N_n are realized using cross adaptors.

Corresponding to the design methods for real coefficients WDFs in Section 2.2, in

this section we discuss direct design methods for complex WDFs. We implement an even-order classical filter as a lattice CWDFs by decomposing it into two complex allpass functions $A_1(z)$ and $A_2(z)$ (Section 3.2). Then each complex allpass function is synthesized from the elementary complex first-degree sections. The elementary sections can be realized by the method of Section 3.3.

$$A_1(z) = \lambda \prod_{k=1}^{M} \frac{z^{-1} - z_k}{1 - z_k^* z^{-1}} = \lambda \prod_{k=1}^{M} \frac{z^{-1} + \beta_k}{1 + \beta_k^* z^{-1}}$$

$$A_2(z) = \lambda^* \prod_{k=1}^{M} \frac{z^{-1} - z_k^*}{1 - z_k z^{-1}} = \lambda^* \prod_{k=1}^{M} \frac{z^{-1} + \beta_k^*}{1 + \beta_k z^{-1}}$$

where λ is a unimodular multiplier.

The corresponding block diagram and the signal flow diagram for the complex multiplier coefficient wave digital filter are given in Figure 3.10 and Figure 3.11.

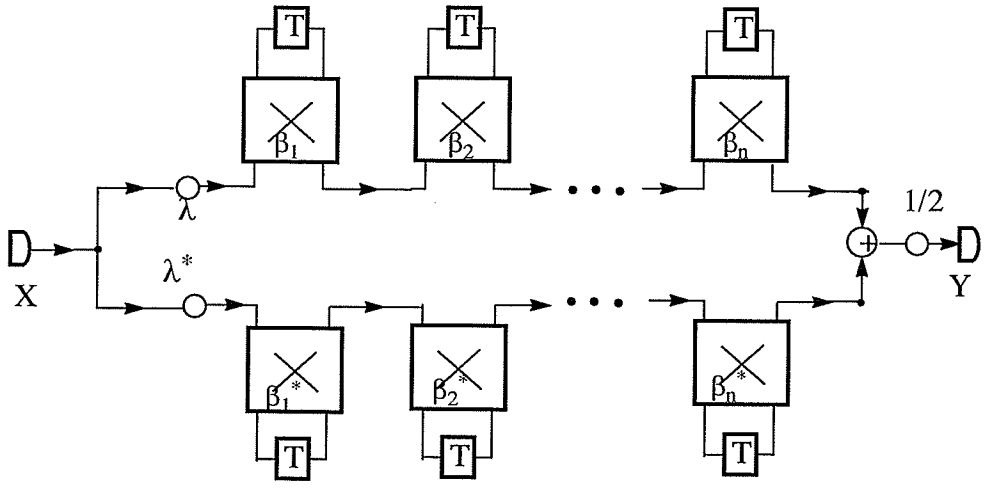

Fig.3.10. Block diagram of complex cross WDF

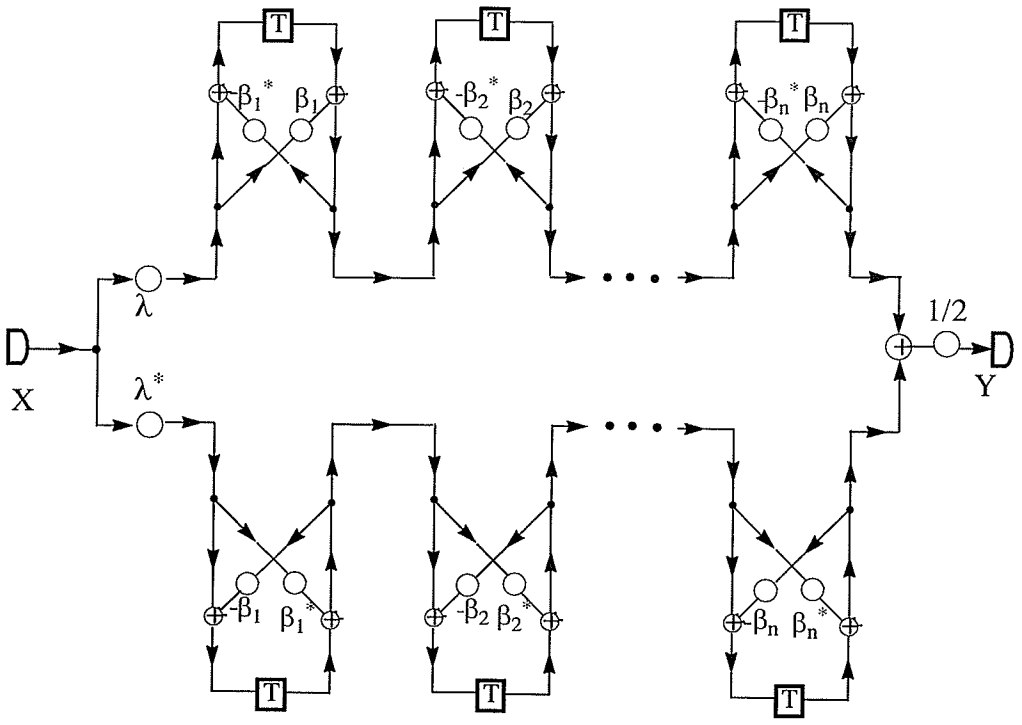

Fig.3.11. Signal-flow diagram of the complex cross WDF.

3.6 The optimization of complex cross adaptor coefficients

In realizing a WDF, we need to quantize the multipliers to a limited number of bits for implementation in hardware. Generally, as the number of bits increases, more accuracy is obtained. However, under the constraint of cost and efficiency, we would like to find the minimal number of bits that could be used to represent the coefficients and preserve as many as possible of the filter's frequency response characteristics (the given specifications). This is carried out by an optimization process that searches through a set of parameters $\{\beta_i\}_{i=1}^{M}$ (which vary within specific ranges to increase or decrease the number of bits) for an approximate design, that has minimal number of bits and satisfies the given

specifications.

First, for each coefficient β_i, let $\hat{\beta}_i \approx \beta_i$ be the number obtained after quantization in b bits, i.e., it is the number obtained when β_i is expressed in binary form with rounding. Then $\hat{\beta}_i$ can be written as the binary fraction $\hat{\beta}_i = \frac{n_i}{2^b} \approx \beta_i$, where n_i and b are integers. Then b is the number of binary bits of n_i and $\hat{\beta}_i$ when they are represented in binary form.

After an approximation of $\{\beta_i\}$ has been computed and with $K = [n_1, n_2, \ldots, n_M]$, we use the finite search algorithm developed by Jarmasz [20] which consists of the following steps:

(1) The bits of $\{\hat{\beta}_i\}$ are varied within specified ranges and those $\{\hat{\beta}_i\}$ that satisfy given specifications are recorded as solutions. Stop if a solution is found.

(2) If no solution is found, then b, the number of bits representing $\hat{\beta}_i$, is increased.

To generate the different parameter sets $\{\tilde{\beta}_i\}$ that vary within specified ranges in (1), we let $\tilde{n}_i$ be the numerator of $\tilde{\beta}_i$ and $\tilde{n}_i = n_i + r_i$ with $r_i \in [-\varepsilon_i, \varepsilon_i]$, $i = 1\,(1)\,M$ where ε_i, $i = 1\,(1)\,M$, are positive integers. The digits r_i are generated by counting from $-\varepsilon_i$ to ε_i. The counting algorithm is presented in Figure 3.12 [20]. Define the offset vector

$$R = [r_1, r_2, \ldots, r_M]$$

The new vector $\tilde{\beta} = [\tilde{\beta}_1, \tilde{\beta}_2, \ldots, \tilde{\beta}_M] = \frac{1}{2^b}\tilde{K}$ can be computed from

$$\tilde{K} = K + R = [n_1 + r_1, n_2 + r_2, \ldots, n_M + r_M]$$

$\tilde{\beta}$ is tested to determine if it satisfies the design specificiations.

From Figure 3.12, it is easy to see that the value for COUNT, when END is reached, is

$$COUNT = \prod_{i=1}^{M} (2\varepsilon_i + 1) = COUNT_{max}$$

There exists a one-to-one correspondence between the integer set

$\{i = 1\,(1)\,COUNT_{max}\}$ and the offset vector R generated by the algorithm in Figure 3.12. To illustrate, consider the case $M = 2, \varepsilon_1 = \varepsilon_2 = 1$. We obtain

$COUNT_{max} = \prod_{i=1}^{2} 3 = 9$ and the correspondence between R and COUNT is shown as Figure 3.13. The numbers r_2, r_1 were generated sequentially using the alogrithm in Figure 3.12. For each offset vector $R = [r_1, r_2]$ generated, a corresponding $\tilde{K} = [\tilde{n_1}, \tilde{n_2}]$ is obtained. The results for $K = [n_1, n_2] = [4, 7]$ are also given in Figure 3.13.

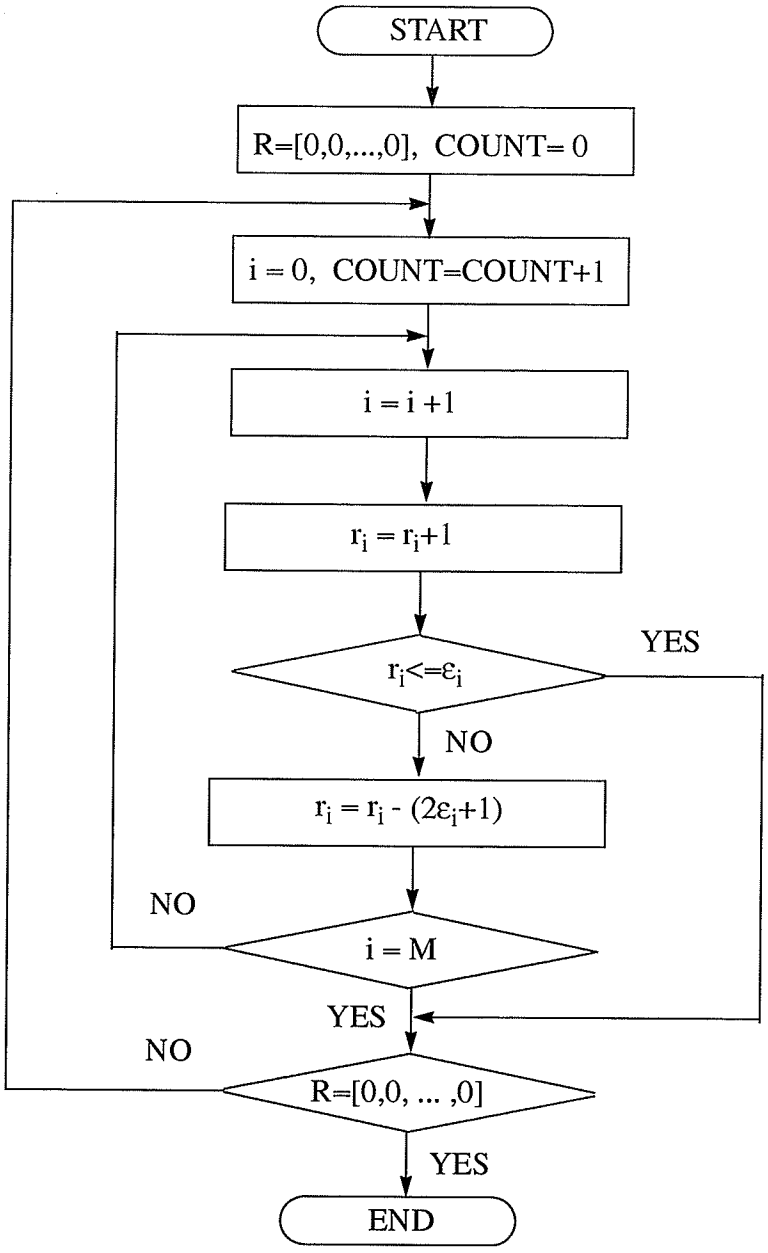

Fig. 3.12 Flowchart for generating all possible R vectors.

COUNT	r_2	r_1	$\tilde{n}_2$	$\tilde{n}_1$
1	0	1	7	5
2	1	-1	8	3
3	1	0	8	4
4	1	1	8	5
5	-1	-1	6	3
6	-1	0	6	4
7	-1	1	6	5
8	0	-1	7	3
9	0	0	7	4

Fig. 3.13. The correspondence between R and COUNT.

It is important to note that, although theoretically it is possible to test all feasible parameter sets, the computer time to do so could be very costly. Consequently, the ranges within which the numbers are allowed to vary must be limited.

Chapter 4

The design procedure and examples

This Chapter presents design procedures for the even-degree classical Butterworth, Chebyshev, and Cauer filters. Design examples are also given to illustrate the procedures.

4.1 The design procedure for complex wave digital filters

We know that explicit formulas exist for WDF realizations of the odd-degree Butterworth, Chebyshev, and Cauer filters, which have already been discussed in [8]. Here, we present similar results for the design of CWDF realizations of the even-degree Butterworth, Chebyshev, and Cauer filters. Namely, explicit formulas and procedures will be given for computing the poles and multiplication coefficients.

The design specifications for a low-pass filter are frequently given in terms of attenuation as illustrated in Figure 4.1, where

A_p : maximum allowable attenuation in the passband in decibels

A_s : specified minimum attenuation in the stopband in decibels

f_s : lower edge frequency of the stopband

f_p : upper edge frequency of the passband

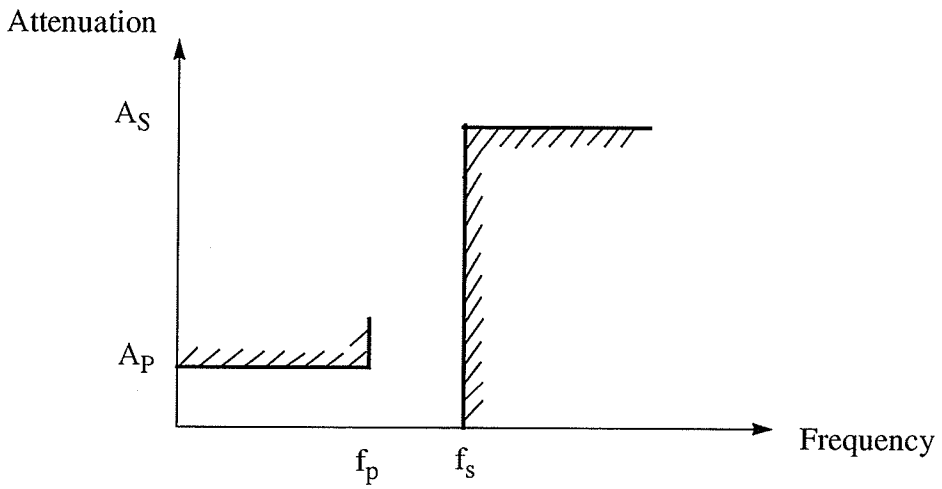

Fig.4.1. Design specifications

F : sampling frequency

Instead of the above parameters, the factors ε_s, ε_p and the transformed frequencies φ_s, φ_p are more convenient in deriving the explicit formulas. They are defined by

$$\varepsilon_s = \sqrt{10^{A_s/10} - 1} \qquad (4.1)$$

$$\varepsilon_p = \sqrt{10^{A_p/10} - 1} \qquad (4.2)$$

φ_s and φ_p are the corresponding analog frequencies obtained via the pre-warping formula which stems from the bilinear transformation (2.7).

$$\varphi_s = \tan(\pi f_s/F) \qquad (4.3)$$

$$\varphi_p = \tan(\pi f_p/F) \qquad (4.4)$$

The first step in the design of a practical filter is the determination of the filter degree n required to meet the above specifications. For the low-pass Butterworth, Chebyshev,

and Cauer filters, a minimum value for the degree can be estimated by using the following approximations [8]:

$$n_{min} = \frac{c_1 \ln (c_2 \cdot \varepsilon_s / \varepsilon_p)}{\ln (c_3)} \qquad (4.5)$$

where c_1, c_2, and c_3 are given in Table 1 with

$$k_0 = \sqrt{\varphi_s / \varphi_p} \qquad (4.6a)$$

and

$$k_{i+1} = k_i^2 + \sqrt{k_i^4 + 1}, \quad \text{for } i = 0, 1, 2, 3. \qquad (4.6b)$$

Table 1:

Filter type	c_1	c_2	c_3
Butterworth	1	1	k_0^2
Chebyshev	1	2	k_1
Cauer	8	4	$2k_4$

Next we describe how to determine the poles and multiplication coefficients for each of the three classical filters. These formulas are deduced from the papers by Darlington [19] and Gazsi [8].

To calculate the poles of a Butterworth Filter

Define the parameters

$$q_0 = \sqrt{\varphi_s / \varphi_p} \qquad (4.7)$$

$$w = 1/\left(q_0 \varepsilon_p^{1/n} \right) \tag{4.8}$$

$$w_{0h} = we^{(i(\delta + h)\pi)/n} \tag{4.9}$$

where $\delta = 0, 1/2$ for n odd, even.

Vary h in equation (4.9) from 1to $2n$, apply the required sequence of transformations and retain the zeros with negative real parts ($\psi_i = w_{0h}$). Then the ψ_i ($i = 1, \ldots, n$) are the poles of $A_1(\psi)$ and $A_2(\psi)$. The poles of the rational functions $A_1(\psi)$ and $A_2(\psi)$ are alternately distributed in a cyclic manner (see Figure 3.4) and hence $A_1(\psi)$ and $A_2(\psi)$ can be determined. For a Butterworth filter $\frac{f}{g}(\infty) = 0$ and $\frac{h}{g}(\infty) = 1$, therefore, from (3.41), $e^{j\theta} = j$. Then, we have

$$A_1(\psi) = e^{j\theta} \prod_{i=1}^{n/2} \frac{\psi + \psi_i^*}{\psi - \psi_i}, \text{ and } A_2(\psi) = e^{-j\theta} \prod_{i=1}^{n/2} \frac{\psi + \psi_i}{\psi - \psi_i^*}.$$

By the bilinear transformation $\psi = \frac{z-1}{z+1}$ (see Section 3.4), $A_1(\psi)$ is transformed from the ψ-plane to the z-plane as $A_1(z)$, and $A_2(\psi)$ is transformed from the ψ-plane to the z-plane as $A_2(z)$.

$$A_1(z) = e^{j\theta} \prod_{i=1}^{n/2} \left(-\frac{\beta_i^* - 1}{\beta_i - 1} \right) \frac{z^{-1} + \beta_i}{1 + \beta_i^* z^{-1}}$$

$$= e^{j\theta} \prod_{i=1}^{n/2} \left(-\frac{\beta_i^* - 1}{\beta_i - 1} \right) \prod_{i=1}^{n/2} \frac{z^{-1} + \beta_i}{1 + \beta_i^* z^{-1}} \tag{4.10a}$$

$$A_2(z) = e^{-j\theta}\prod_{i=1}^{n/2}\left(-\frac{\beta_i - 1}{\beta_i^* - 1}\right)\frac{z^{-1} + \beta_i^*}{1 + \beta_i z^{-1}}$$

$$= e^{-j\theta}\prod_{i=1}^{n/2}\left(-\frac{\beta_i - 1}{\beta_i^* - 1}\right)\prod_{i=1}^{n/2}\frac{z^{-1} + \beta_i^*}{1 + \beta_i z^{-1}} \qquad (4.10b)$$

Define

$$\lambda = e^{j\theta}\prod_{i=1}^{n/2}\left(-\frac{\beta_i^* - 1}{\beta_i - 1}\right) \qquad (4.11)$$

Then

$$A_1(z) = \lambda\prod_{i=1}^{n/2}\frac{z^{-1} + \beta_i}{1 + \beta_i^* z^{-1}}, \text{ and } A_2(z) = \lambda^*\prod_{i=1}^{n/2}\frac{z^{-1} + \beta_i^*}{1 + \beta_i z^{-1}}$$

where

$$\beta_i = \frac{\psi_i^* + 1}{\psi_i^* - 1}$$

are the cross adaptor coefficients, $i = 1, \ldots, n/2$.

To calculate the poles of a Chebyshev Filter

Define the parameters

$$q_0 = \sqrt{\varphi_s/\varphi_p} \qquad (4.12a)$$

$$w = \sqrt[n]{\frac{1}{\varepsilon_p} + \sqrt{\frac{1}{\varepsilon_p^2} + 1}} \qquad (4.12b)$$

$$w_{1h} = we^{(i(\delta + h)\pi)/n} \qquad (4.12c)$$

where $\delta = 0, 1/2$ for n odd, even.

$$w_{0h} = \frac{1}{2q_0}\left(w_{1h} - \frac{1}{w_{1h}}\right) \qquad (4.13)$$

Vary h in equation (4.12) from 1to $2n$, apply the required sequence of transformations and retain the zeros with negative real parts ($\psi_i = w_{0h}$). Then, the same as above, determine the poles of $A_1(\psi)$, $A_2(\psi)$ using the alternating distribution property. Finally, using the bilinear transformation transfer the poles from the ψ-domain to the z-domain to get the cross adaptor coefficients β_i, $i = 1, \ldots, n/2$; $e^{j\theta}$ and λ are determined as for a Butterworth filter.

To calculate the poles of a Cauer Parameter (elliptic) Filter

$$q_0 = \sqrt{\varphi_s/\varphi_p} \qquad (4.14a)$$

$$q_{i+1} = q_i^2 + \sqrt{q_i^4 - 1}, \text{ for } i = 0, 1, 2, 3 \qquad (4.14b)$$

$$m_4 = \frac{1}{2}(2q_4)^n \qquad (4.15a)$$

$$m_{i-1} = \sqrt{\frac{1}{2}\left(m_i + \frac{1}{m_i}\right)}, \text{ for } i = 4, 3, 2, 1 \qquad (4.15b)$$

and furthe, define auxiliary parameters by means of

$$g_1 = \frac{1}{\varepsilon_p} + \sqrt{\frac{1}{\varepsilon_p^2} + 1} \qquad (4.16a)$$

$$g_{i+1} = m_i g_i + \sqrt{(m_i g_i)^2 + 1}, \text{ for } i = 0, 1, 2, 3 \qquad (4.16b)$$

$$w_{50} = \sqrt[N]{\frac{m_4}{g_4} + \sqrt{\left(\frac{m_4}{g_4}\right)^2 + 1}} \qquad (4.17)$$

$$w_5 = w_{50} e^{(i(\delta + h)\pi)/n} \qquad (4.18)$$

where $\delta = 0, 1/2$ for n odd, even.

$$w_{i-1} = \frac{1}{2q_{i-1}}\left(w_i - \frac{1}{w_i}\right), \text{ for } i = 5, 4, 3, 2, 1 \qquad (4.19)$$

Vary h in equation (4.18) from 1to $2n$, apply the required sequence of transformations and retain the zeros with negative real parts ($\psi_i = w_{0h}$). Then, as for a Butterworth filter determine the poles of $A_1(\psi)$, $A_2(\psi)$ using the alternating distribution property. To calculate $e^{j\theta}$ of a Cauer filter, the transmission zeros are required.

To calculate the transmission zeros

$$y_{4k} = \frac{q_4}{\cos\left(\frac{k\pi}{n2}\right)}, \text{ for } k = 0 \text{ to } n-1. \qquad (4.20a)$$

$$w_k = y_{0k}\sqrt{\varphi_s \varphi_p} \qquad (4.20b)$$

where w_k is a transmission zero.

In [25], Saal presented two cases for the frequency response: case a and case b. In case a, we obtain $\frac{f}{g}(\infty) = \frac{1}{\sqrt{1 + k_h^2}}$ and $\frac{h}{g}(\infty) = \frac{k_h}{\sqrt{1 + k_h^2}}$, where $k_h = \frac{\varepsilon_p m_0 |f(0)|}{q_0^n}$ and $|f(0)|$ is the product of all the zeros of f. From (3.41) $e^{j\theta} = \frac{f}{g}(\infty) + \frac{h}{g}(\infty)$. Then

we have $A_1(\psi) = e^{j\theta}\prod_{i=1}^{n/2}\frac{\psi+\psi_i^*}{\psi-\psi_i}$, and $A_2(\psi) = e^{-j\theta}\prod_{i=1}^{n/2}\frac{\psi+\psi_i}{\psi-\psi_i^*}$. Finally, by the bilinear transformation transfer the poles from ψ-plane to z-plane to get the cross adaptor coefficients β_i, $i = 1, \ldots, n/2$.

In case b, the largest transmission zero w_{max} in (4.20b) and its complex conjugate are transformed to infinity, and the remaining zeros of f and the zeros of g are transformed with the formula [25]

$$\tilde{\psi}^2 = \frac{\left(w_{max}^2 - 1\right)\psi^2}{w_{max}^2 + \psi^2} \qquad (4.21)$$

where ψ and $\tilde{\psi}$ are the complex frequencies of cases a and b, respectively. And $\frac{f}{g}(\infty) = 0$, $\frac{h}{g}(\infty) = 1$ and $e^{j\theta} = j$. The rest of the design procedure is the same as in case a. The frequency response of Example 3 is an example of case b.

4.2 The design examples

In this section, we present examples illustrating the above procedure. The optimization process of Section 3.6 is also used.

Example 1: a Butterworth filter. The design specifications are as follows:

Passband: $f_p = 4.0$ kHz $\quad A_p = 0.1$ dB

Stopband: $f_s = 6.06$ kHz $\quad A_s = 40$ dB

Sampling frequency: $F = 16$ kHz.

From Section 3.5 $A_1(z) = \lambda \prod_{k=1}^{M} \frac{z^{-1} + \beta_k}{1 + \beta_k^* z^{-1}}$, and $A_2(z) = \lambda^* \prod_{k=1}^{M} \frac{z^{-1} + \beta_k^*}{1 + \beta_k z^{-1}}$.

In this example, $M = n/2 = 4$

First, we get all the coefficients using (4.11) and (4.7)-(4.9) as follows:

$$\lambda = 0.79255208 - j0.60980423$$

$$\beta_1 = 0.19393093 + j0.80206562$$

$$\beta_2 = 0.12755109 + j0.29882163$$

$$\beta_3 = 0.11806879 - j0.97131420$$

$$\beta_4 = 0.14977756 - j0.52514838$$

Second, choosing 6 bits for the quantized coefficients, yields:

$$\lambda = 50/64 - j39/64$$

$$\beta_1 = 12/64 + j51/64$$

$$\beta_2 = 8/64 + j19/64$$

$$\beta_3 = 7/64 - j6/64$$

$$\beta_4 = 9/64 - j33/64$$

The frequency response for the quantized system is shown in Figure 4.2. We note that the transmission zero has shifted from $f/F = 0.5$ to $f/F = 0.4$ due to quantization and the level in the passband has shifted up by 0.08 dB due the quantization of the unimodular multiplier. Also, for 6 bits of quantization the design specifications are not satisfied. The optimized 6-bit coefficients are as follows:

$$\lambda = 51/64 - j38/64$$

$$\beta_1 = 13/64 + j52/64$$

$$\beta_2 = 8/64 + j19/64$$

$$\beta_3 = 7/64 - j6/64$$

$$\beta_4 = 9/64 - j33/64$$

The frequency response for the optimized system is shown in Figure 4.3; the design specifications are satisfied after optimization. The corresponding WDF diagram is shown in Figure 3.10 and Figure 3.11.

Example 2, a Chebyshev filter, the design specifications are as follows:

Passband: $f_p = 4.0$ kHz $\quad A_p = 0.1$ dB

Stopband: $f_s = 5.0$ kHz $\quad A_s = 40$ dB

Sampling frequency: $F = 16$ kHz.

From Section 3.5, $A_1(z) = \lambda \prod_{k=1}^{M} \frac{z^{-1} + \beta_k}{1 + \beta_k^* z^{-1}}$, and $A_2(z) = \lambda^* \prod_{k=1}^{M} \frac{z^{-1} + \beta_k^*}{1 + \beta_k z^{-1}}$.

In this example, $M = n/2 = 4$

First, we get all the coefficients using (4.11) and (4.12), (4.13) as follows:

$$\lambda = 0.72977057 - j0.68369212$$

$$\beta_1 = 0.31623816 + j0.93943470$$

$$\beta_2 = -0.29761296 + j0.59613754$$

$$\beta_3 = -0.47760190 - j0.22954025$$

$$\beta_4 = -0.92962980 - j0.80898964$$

Choosing 10 bits of quantization for the coefficients, gives the following:

$$\lambda = 747/1024 - j700/1024$$

$$\beta_1 = 32/1024 + j961/1024$$

$$\beta_2 = -304/1024 + j610/1024$$

$$\beta_3 = -489/1024 - j235/1024$$

$$\beta_4 = -95/1024 - j828/1024$$

The frequency response for the quantized system is shown in Figure 4.4. We note that the transmission zero has shifted from $f/F = 0.5$ to $f/F = 0.44$ due to quantization. Also, for 10 bits of quantization the design specifications are not satisfied. The optimized coefficients of length 10 bits follow:

$$\lambda = 748/1024 - j699/1024$$

$$\beta_1 = 33/1024 + j962/1024$$

$$\beta_2 = -305/1024 + j609/1024$$

$$\beta_3 = -488/1024 - j234/1024$$

$$\beta_4 = -95/1024 - j828/1024$$

The frequency response for the optimized system is shown in Figure 4.5; the design specifications are satisfied after optimization. The corresponding WDF diagram is shown in Figure 3.10 and Figure 3.11.

Example 3, a Cauer filter, the design specifications from [10] are as follows:

Passband: $f_p = 3.4$ kHz, $A_p = 0.1$ dB

Stopband: $f_s = 4.6$ kHz, $A_s = 80$ dB

Sampling frequency: $F = 16$ kHz.

From section 3.5, $A_1(z) = \lambda \prod_{k=1}^{M} \frac{z^{-1} + \beta_k}{1 + \beta_k^* z^{-1}}$, and $A_2(z) = \lambda^* \prod_{k=1}^{M} \frac{z^{-1} + \beta_k^*}{1 + \beta_k z^{-1}}$.

In this example, $M = n/2 = 4$

Using (4.20), (4.21), the transmission zeros are as follows:

$f_1 = 0.0000000 + j1.3010445$, $f_2 = 0.0000000 + j1.5002911$

$f_3 = 0.0000000 + j2.2277880$, $f_4 = 0.0000000 - j1.3010445$

$f_5 = 0.0000000 - j1.5002911$, $f_6 = 0.0000000 - j2.2277880$

Using (4.14)-(4.19), the zeros of g are as follows:

$g_1 = -0.21338281 + j0.50348335$, $g_2 = -0.12278124 + j0.70965761$

$g_3 = -0.03885768 + j0.80445136$, $g_4 = -0.28032632 + j0.18499087$

$g_5 = -0.21338281 - j0.50348335$, $g_6 = -0.12278124 - j0.70965761$

$g_7 = -0.03885768 - j0.80445136$, $g_8 = -0.28032632 - j0.18499087$

Finally, we get all the coefficients using (4.11), (4.20), (4.21) and the bilinear transformation applied to the zeros of f and g:

$\lambda = 0.63664746 - j0.77115497$

$\beta_1 = -0.40617395 + j0.58348068$

$\beta_2 = -0.20351874 + j0.93195854$

$$\beta_3 = -0.27281303 - j0.80448570$$

$$\beta_4 = -0.53015731 - j0.22108827$$

Choosing 12-bit coefficients, the quantized coefficients are as follows:

$$\lambda = 2607/4096 - j3158/4096$$

$$\beta_1 = -1663/4096 + j2389/4096$$

$$\beta_2 = -833/4096 + j3817/4096$$

$$\beta_3 = -1117/4096 - j3295/4096$$

$$\beta_4 = -2171/4096 - j905/4096$$

The frequency response for the quantized system is shown in Figure 4.6. We note that for 12 bits of quantization the design specifications are not satisfied. The optimized coefficients of length 12 bits are as follows:

$$\lambda = 2607/4096 - j3159/4096$$

$$\beta_1 = -1664/4096 + j2388/4096$$

$$\beta_2 = -833/4096 + j3817/4096$$

$$\beta_3 = -1117/4096 - j3295/4096$$

$$\beta_4 = -2170/4096 - j904/4096$$

The frequency response for the optimized system is shown in Figure 4.7, the design specifications are satisfied after optimization. The corresponding WDF diagram is shown in Figure 3.10 and Figure 3.11.

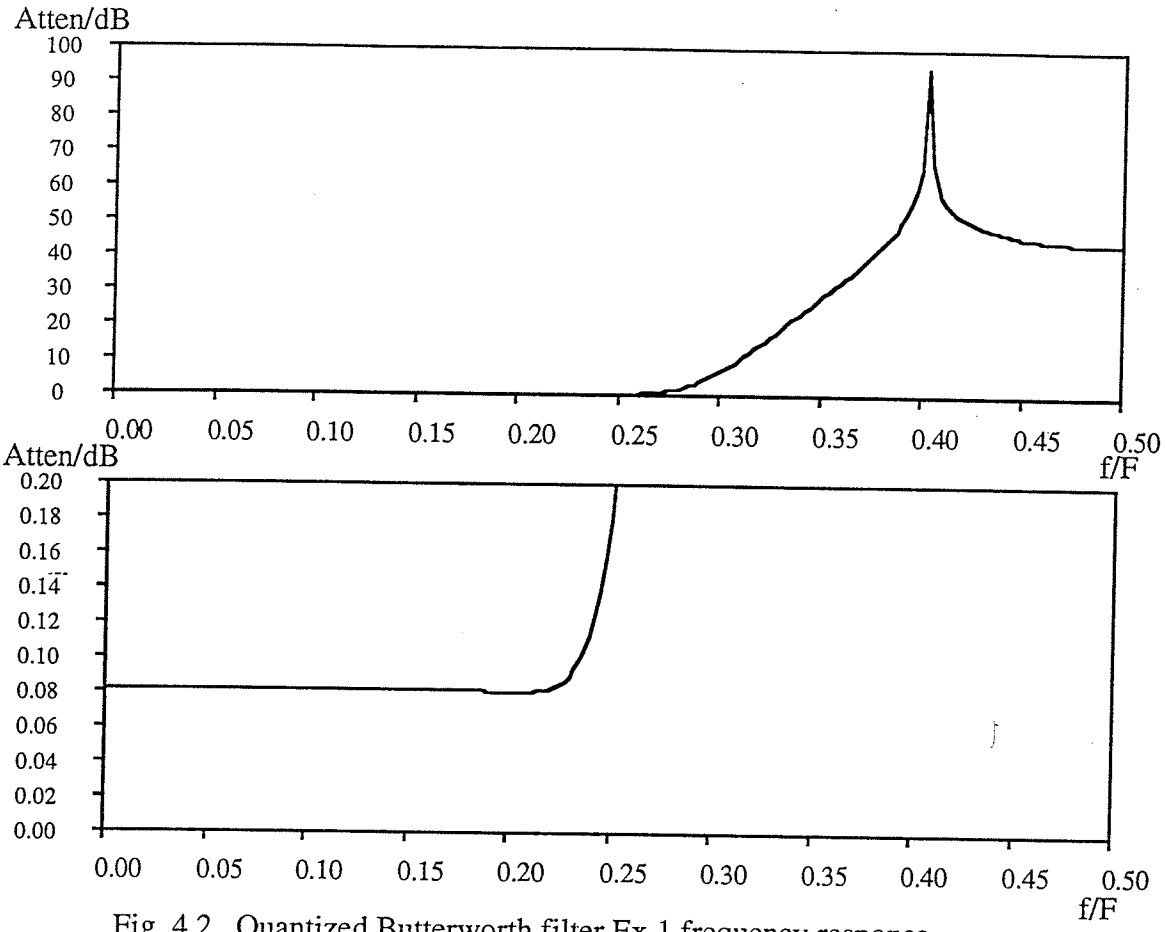

Fig. 4.2 . Quantized Butterworth filter Ex 1 frequency response.

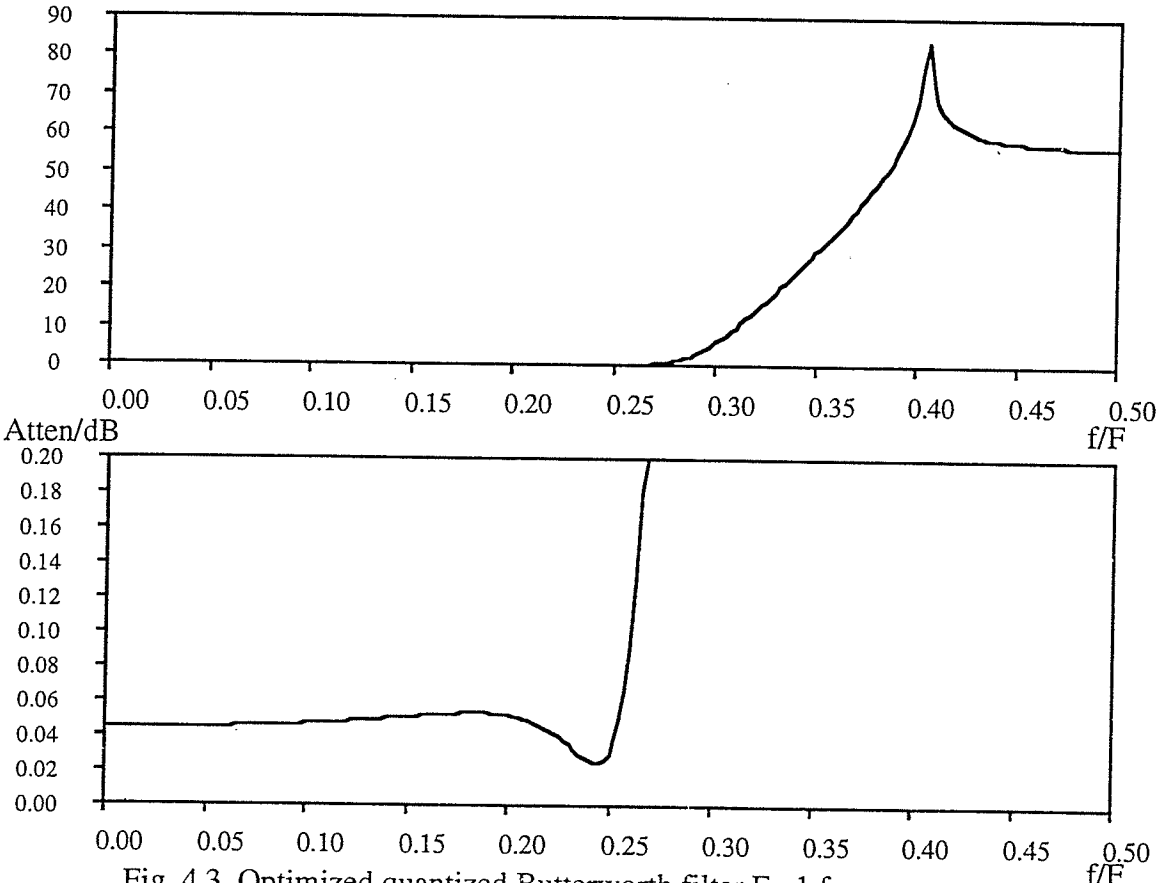

Fig. 4.3. Optimized quantized Butterworth filter Ex 1 frequency response.

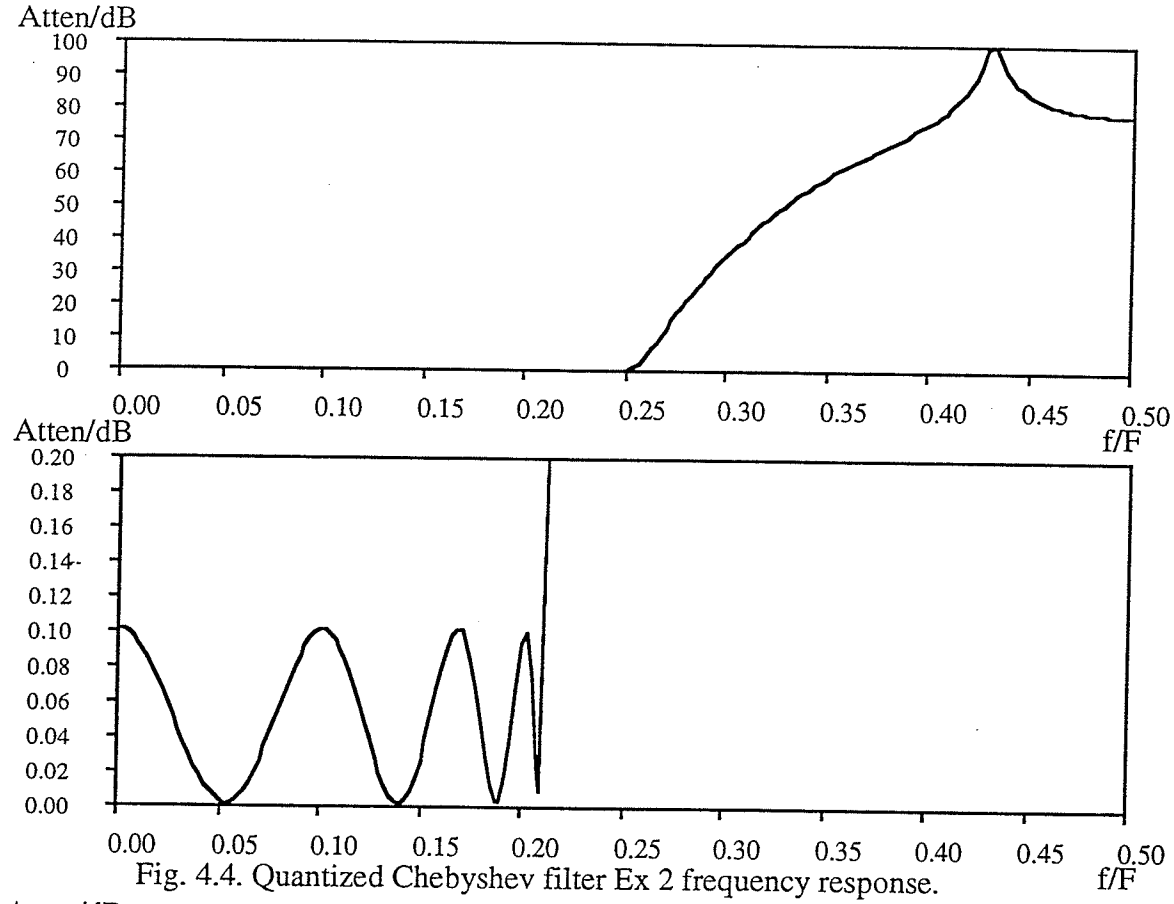

Fig. 4.4. Quantized Chebyshev filter Ex 2 frequency response.

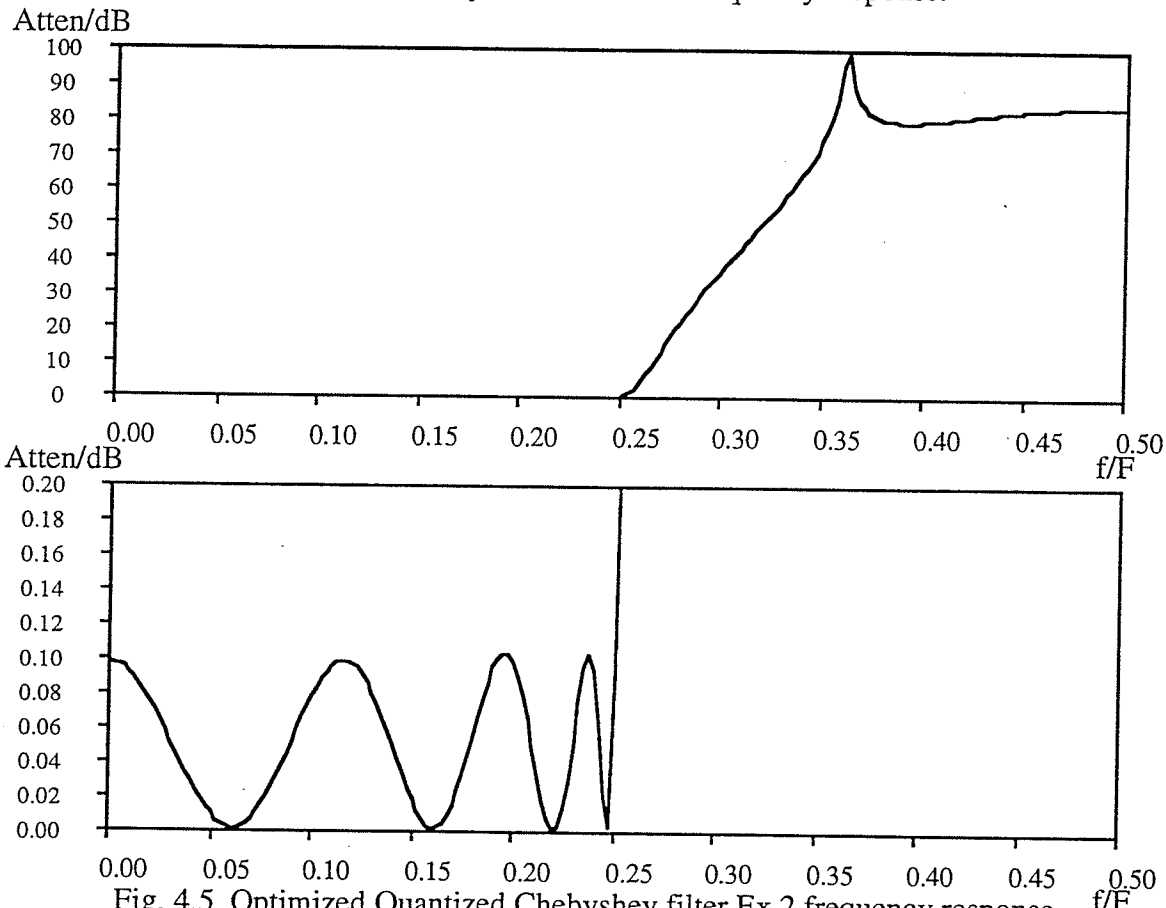

Fig. 4.5. Optimized Quantized Chebyshev filter Ex 2 frequency response.

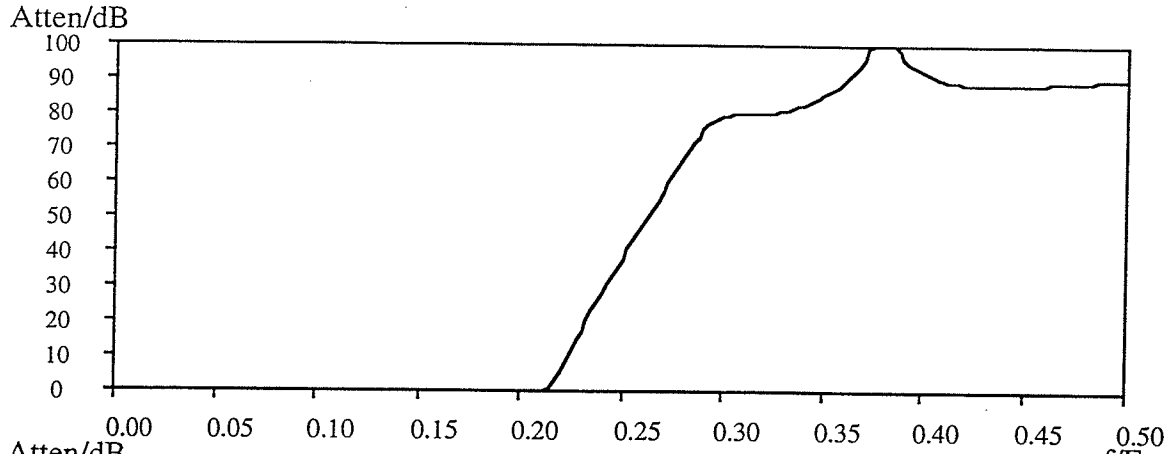

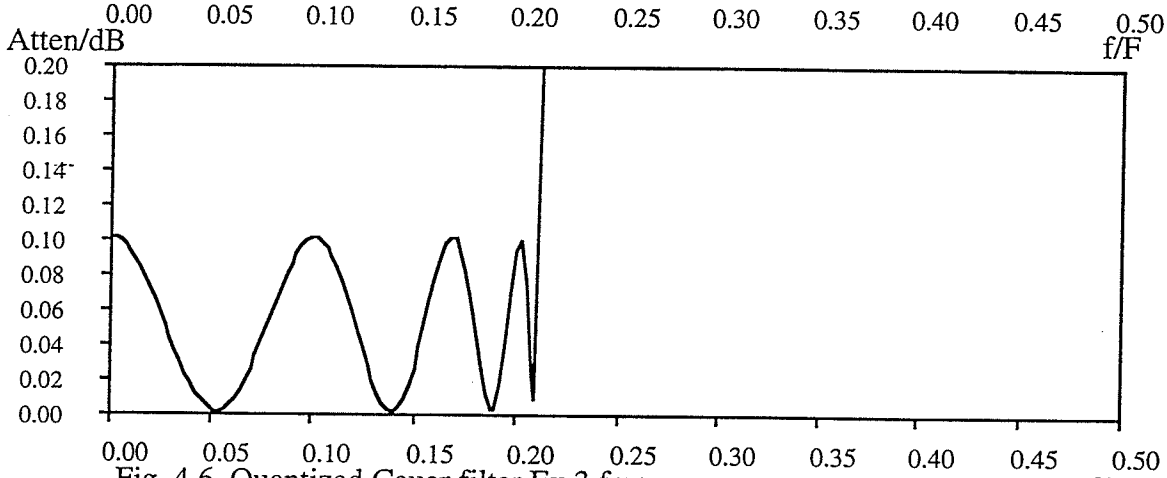

Fig. 4.6. Quantized Cauer filter Ex 3 frequency response.

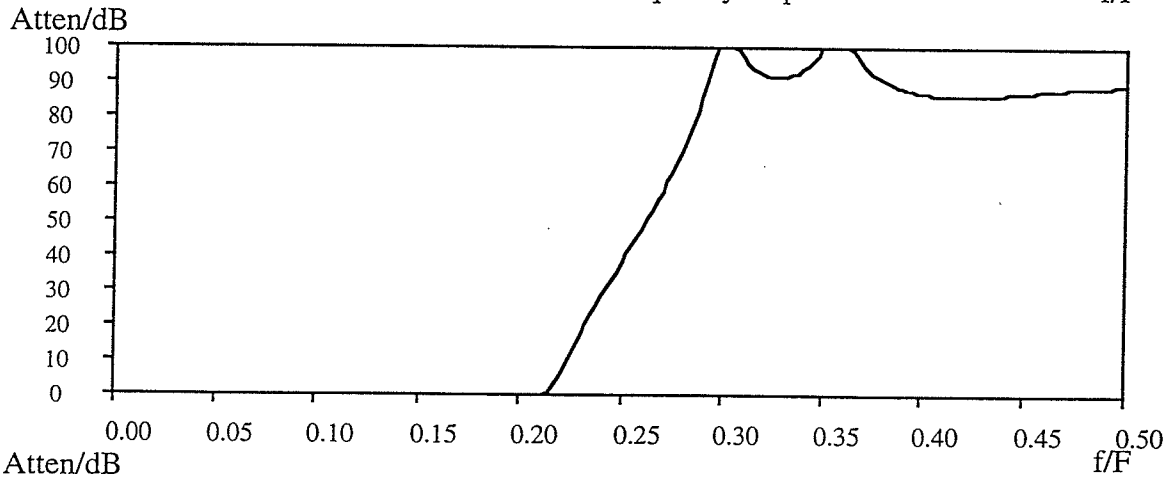

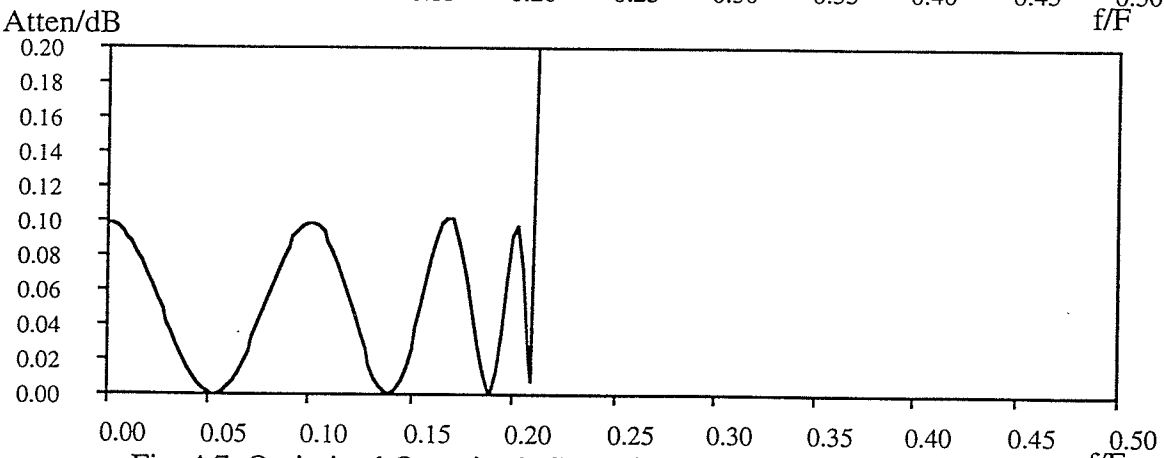

Fig. 4.7. Optimized Quantized Cauer filter Ex 3 frequency response.

Chapter 5

Conclusions

A complex lattice WDF realization of even-order classical lowpass filters such as Butterworth, Chebyshev and Cauer filters has been given. Complex first-degree allpass sections are implemented by a complex two-port cross adaptor with a delay. The cross adaptor represents an implementation of a first-degree section with two complex multipliers and a delay, but the two multipliers differ from each other only in the sign of their real parts and must have a magnitude less than unity. So essentially, there is only one coefficient involved. Also, the complex wave digital adaptor can be implemented with a real wave digital adaptor and a unimodular multiplier. With the explicit formulas available, the design process is simple and parallel to the one for the WDF realization of odd-order classical lowpass filters [8]. The design examples confirm the effectiveness of optimizing the wordlength.

For future work, it remains to be explored whether first-degree complex allpass sections can be implemented with one complex multiplier and one delay. (For allpass functions with real coefficients, the lattice structure with one multiplier and one delay per section are well known). This will make it comparable with the realization of odd-order filters.

References

[1] A. Fettweis, "Wave digital filters: theory and practice", *Proc. IEEE*, vol. 74, pp. 270-327, Feb. 1986.

[2] A. Fettweis, "Digital filter structures related to classical filter networks", *Arch.Elek. Übertragung*, vol. 25, pp. 79-89, Feb.1971.

[3] G. Scarth and G. O. Martens, "Complex wave digital networks using complex port references", *Proc. IEEE Inter. Conf. on ASSP.* (Glasgow, Scotland, May. 1989), vol. 2, pp 841-844.

[4] G. Scarth, "Complex wave digital networks including the implementation of even-order filters", M. Sc. Thesis, University of Manitoba, Winnipeg, Manitoba, Canada, 1988.

[5] A. Fettweis, "Principles of complex wave digital filters", *Int. J. Circuit Theory Appl.*, vol. 9, pp. 119-134, Apr. 1981.

[6] G. O. Martens, Private communication.

[7] K. Meerkötter, "Complex passive networks and wave digital filters", in *Proc. Eur. Conf. on Circuit Theory and Design* (Warsaw, Poland, Sept. 1980), vol. 2, pp. 24 -35.

[8] L. Gazsi, "Explicit formulas for lattice wave digital filters", *IEEE Trans. Circuits and Syst.*, vol. CAS-32, pp.68-88, Jan. 1985.

[9] P. P. Vaidyanathan, P. P. Regalia, and S. K. Mitra, "Design of double-complemenary IIR digital filters using a single complex allpass filter, with multirate applications", *IEEE Trans. Circuits and Syst.*, vol. CAS-34, no. 4, pp. 378-389, Apr. 1987.

[10] H. D. Schütte "On adaptors for complex wave digital filters", in *Proc. IEEE International Symposium on Circuits and System,* 1989, vol. 3, pp. 1644-1674.

[11] P. P. Regalia, S. K. Mitra and J. Fadavi-Ardekani, "Implementation of real coefficient digital filter using complex arithmetic", *IEEE Trans. Circuits and Syst.* vol. CAS-34, no. 4, pp. 345-353, Apr. 1987.

[12] P. P. Regalia, S. K. Mitra, "Low-sensitivity active filter realization using a complex all-pass filter", *IEEE Trans. Circuits and Syst.*, CAS-34, no. 4, pp. 390-399, Apr. 1987.

[13] T. H. Crystal and L. Ehrman, "The design and applications of digital filters with complex coefficients", *IEEE Trans. On Audio and Electroacoustics,* vol. AU-16, No. 3, Sept. 1968.

[14] P. P. Vaidyanathan, S. K. Mitra, and Y. Neuvo, "A New approach to the realization of low-sensitivity IIR digital filters", *IEEE Trans. on Acoust., Speech, Singal Processing*, vol. ASSP-34, No. 2, pp. 3350-361. Apr. 1986.

[15] A. Fettweis, H. Levin, and A. Sedlmeyer, "Wave digital lattice filters", *Int. J. Circuit Theory Appl.,* vol. 2, no. 2, pp. 203-211, June 1974.

[16] A. H. Gray and J. D. Markel, "Digital lattice and ladder filter synthesis", *IEEE Trans. Audio Electroacoustics,* vol. AU-21, pp. 491-500, Dec. 1973.

[17] G. Scarth and G. O. Martens, "Complex wave digital ladder filters using complex port references", in *proc. IEEE International Symposium on Circuits and System,* (Singapore, June 1991), vol. 5, pp. 2447-2450.

[18] K. Meerkötter, "Antimetric wave digital filters derived from complex reference circuits", *Proc. Eur. Conf. on Circuit Theory and Design* (Stuttgart, W. Germany,

Sept.1983).

[19] S. Darlington, "Simple algorithms for elliptic filters and generalizations thereof," *IEEE Trans. Circuits Syst.*, vol. CAS-25, pp. 975-980, Dec.1978.

[20] M. R. Jarmasz, "Design of canonic wave digital filters which suppress all zero-input parasitic oscillations", M. Sc. Thesis, University of Manitoba, Winnipeg, Manitoba, Canada, 1983.

[21] V. W. T. Cheng, "Synthesis of modular and pipelineable wave digital filters", M. Sc. Thesis, University of Manitoba, Winnipeg, Manitoba, Canada, 1992.

[22] A. Fettweis, "Pseudopassivity, sensitivity, and stability of wave digital filters", *IEEE Trans. Circuit Theory*, vol. CT-19, pp. 668-673, Nov. 1972.

[23] A. Fettweis, "Scattering properties of real and complex lossless two-ports", *Proc. IEE*, vol.128, Pt. G, No. 4, Aug. 1981.

[24] V. Belevitch, *Classical Network Theory*, San Francisco, CA: Holden-day, 1968.

[25] R. Saal, *Handbook of Filter Design*, Berlin; Frankfurt, am Main, 1979.